Journal of Archaeological Science: Reports 54 (2024) 104408

Contents lists available at ScienceDirect

Journal of Archaeological Science: Reports

journal homepage: www.elsevier.com/locate/jasrep

Variability and temporality of lithic production in Epipaleolithic to Early Neolithic occupations at Cova del Vidre (Catalonia, Spain)

Ivan Gironès-Rofes [a,*], Josep Bosch-Argilagós [b], Anna Bach-Gómez [a], Miquel Molist [a], Salvador Pardo-Gordó [c]

[a] SAPPO-GRAMPO, Department of Prehistory, Autonomous University of Barcelona, Spain
[b] Museu de Gavà, Spain
[c] Departamento de Geografía e Historia, Universidad de la Laguna, Spain

ARTICLE INFO

Keywords:
Cova del Vidre
Lithic industry
Epipaleolithic
Late Mesolithic
Early Cardial Neolithic
Iberian peninsula
El Port massif
Ebro River

ABSTRACT

Cova del Vidre (Roquetes, Tarragona, Spain), strategically located in El Port massif, a high-altitude mountain range contrasting with the lower course of the Ebro River, has an interrupted sequence of occupations from the beginning of the Holocene until the establishment of the first Neolithic groups (c. 10,800–5000 cal. BC). It is currently the site with the most complete sequence detected in the lower Ebro valley.

The comprehensive analysis of the knapped lithic industry from the four phases identified during excavations in the 1950s–1960s and 1992 (Microlaminar Epipaleolithic, Sauveterrian, Late Mesolithic, and Early Cardial Neolithic) reveals significant evolution in the management and exploitation of chipped stone raw materials, their technology, and the formalization of tools in the four occupation phases. Furthermore, the chronological determination of the Sauveterrian phase by radiocarbon dating (14C) allows us to integrate the largest assemblage in the sequence within the regional productive dynamics. It also enables us to establish the temporal sequence of the detected occupations together with the previously published radiocarbon dates.

1. Introduction

Cova del Vidre is a key site with recurrent occupation in the lower Ebro River basin. Its location makes it a strategic site due to its proximity to resources, and its role as a refuge on route networks and for controlling the surrounding valleys. As a result, it was frequented by human groups throughout recent prehistory. Four main phases of occupation have been identified in this archaeological deposit: Microlaminar Epipaleolithic, Sauveterrian, Late Mesolithic, and Early Cardial Neolithic (c. 10,800–5000 cal. BC). Of these phases, the Sauveterrian phase has not been dated until now, which has hindered the integration of its data into the peninsular Sauveterrian lithic industries (Soto et al., 2016, 2020; Román & Domingo, 2019).

At the same time, the Late Mesolithic (6800–5700 cal. BC) represents a widespread gap in the northeastern Iberian Peninsula due to the great scarcity of known occupations. In addition, there is the indefiniteness of its lithic assemblages in the northeastern Iberian Peninsula, as has been discussed in numerous studies (Barceló, 2008; Vaquero & García-Argüelles, 2009; Morales & Oms, 2012; Morales et al., 2013a; Juan-Cabanilles & Martí, 2002; Juan-Cabanilles & García-Puchol, 2013; Oms et al., 2017; among others). This gap has also been detected in the border area of the Ebro basin, which makes the site discussed in this study one of the few that can present geometric elements linked to this period. Nevertheless, the site does not integrate within the lithic production dynamics of Lower Aragon (Utrilla et al., 2009) or central-southern Valencia (Martí et al., 2009). The lithic assemblage dated between 6300 and 6000 cal. BC in Cova del Vidre does not allow for differentiation in any of the sub-phases based on the proportions of trapezoidal geometric arrowheads and the sparse presence of triangles (Phase A) or the predominant presence of triangles over trapezoids (Phase B) including the characteristic Cocina-type triangle (triangle with two concave edges and a generally rounded vertex) (Fortea, 1971, 1973; Juan-Cabanilles, 1985).

Within the dynamics of the prehistoric population in this area, cave occupations characterize the Epipaleolithic periods in the lower Ebro region through Cova del Clot de l'Hospital (Bosch et al., 2015; Bosch, 2011, 2016a, 2016b), and Cova del Vidre, which includes Sauveterrian industries, limited geometric elements from the Late Mesolithic, and

* Corresponding autor at: Edifici MRA – Campus de la UAB, 08193 Bellaterra, Spain.
E-mail address: ivan.girones@uab.cat (I. Gironès-Rofes).

https://doi.org/10.1016/j.jasrep.2024.104408
Received 1 August 2023; Received in revised form 13 January 2024; Accepted 18 January 2024
Available online 1 February 2024

Cardial Neolithic pottery production (Bosch, 2011, 2016a, 2016b; Bosch et al., 2022). Later, prehistoric data proliferates for the Epicardial period on the Ebro river terraces (El Molló, Piera et al., 2016; Barranc d'en Fabra, Bosch, 1993, Bosch et al., 1996; Riols I, Royo & Gómez, 1992), and there is extensive surface material evidence that indicates open-air occupations or activities on the terraces throughout the valley (Genera, 1991, 1993; Esteve Gálvez, 2000; Bosch, 2005; Molist et al., 2020; Gironès et al., 2020; Gironès & Molist, 2023), but not in caves. The lithic technocomplexes at Cova del Vidre provide valuable information about production during this transition in the area, albeit fragmented due to the lack of new stratified sites.

Although some general information is available about these lithic industries (Bosch, 2001; Bosch, 2005; Bosch, 2016a), we lack a detailed diachronic understanding of the productive changes in this micro-region, as well as their relationships and differences beyond this territorial framework, which would allow us to integrate them into regional productions.

To evaluate the changes systematically and fully in the exploitation and management of lithic productions in the occupations of Cova del Vidre, this study presents an analysis of the contextualized lithic assemblages from the levels reliably assigned to the four identified chrono-cultural phases. It focuses on an initial approach to the management of raw materials, their exploitation, and transformation into tools, together with a new radiocarbon date that establishes the chronology of the assemblage associated with the Sauveterrian, which is the most abundant one at the site. The main objectives are to determine a more rigorous productive and chronological delimitation of the contextualized lithic assemblages through their revision and systematization, as well as to implement new radiocarbon dating that can provide a more precise temporal framework. This will generate reliable information for further analysis and integration into the macro-regional lithic productive dynamics within each chrono-cultural horizon.

2. Cova del Vidre

2.1. Cova del Vidre location

Cova del Vidre (UTM ETRS89 31N X: 273426.8, Y: 4517063.3) is in the mountainous unit of El Port massif, in the modern village of Roquetes (Baix Ebre, Tarragona) (Fig. 1). The cave is oriented east-northeast in the limestone wall of the southeast slope of Mola del Boix, at an approximate altitude of 1,020 m above sea level and about 4 km in a straight line from the summit of Caro (1,447 m above sea level). Its location is optimal on a mountain pass connecting the high plateaus in the surrounding area. It offers a wide panoramic view of the network of valleys and ravines that flow into the secondary waterways of Barranc de Barretes and Barranc de Lloret, extending to the plain of the Ebro basin and the delta. The cave has a triangular-shaped entrance in a fold in the limestone wall, approximately 30 m wide and 15 m high, while the ceiling descends gradually towards the deepest part. Inside, there are two adjoining chambers: a main chamber with a depth of 43 m, characterized by large blocks detached from the ceiling, and a second space in the northern wall, measuring 15 m in length, 10 m in width, and with a height of just over 1.5 m due to sedimentological infilling from the main chamber.

2.2. Archaeological context and past fieldwork

As described in recently published studies (Bosch, 2001, 2005, 2016a), the first archaeological fieldwork at the site was conducted by Francesc Esteve Gálvez in 1945, with two trenches: one inside the cave and the other in the central-northern area. The lithic remains that were recovered indicated Neolithic and Upper Paleolithic levels in the first trench. Subsequently, in 1954, Esteve Gálvez performed a second excavation in the same areas, expanding the recovered material assemblages from the previously identified occupation phases. In 1957, 1958, and 1960, Ignasi Cantarell carried out several excavations inside the cave, further enhancing the stratigraphic information acquired by Esteve Gálvez. Cantarell's work focused on excavating six trenches in the main chamber and one in the small adjoining inner chamber to the north. In 1957, Cantarell excavated test pits A, B, and C, documenting Neolithic and Epipaleolithic levels. According to Cantarell's original documents, between 1957 and 1958, Esteve Gálvez performed his last excavation between test pits A and C, leading Cantarell to intervene in the same area in 1960 (referred to as test pit E and the "Esteve Zone"), as well as recovering surface material in the Central Zone of the main chamber.

Stratigraphically, Cantarell defined three levels (EI, unidentified *in situ*, EII, and EIII) in Esteve's test pit E and the so-called "Esteve Zone," which consisted of sediments extracted by F. Esteve Gálvez. The last two layers (EII and EIII) were assigned to the Early Neolithic horizon due to the presence of pottery sherds. In Cantarell's new excavations, the following sequence was recorded (Bosch, 2016a): Trench A with five levels (A1-A5), Trench B with two levels (B1 and B2), and Trench C with six levels (C1-C6). Initially, these levels were classified as belonging to the Early Neolithic (C1, B1, B2, A1, A2, and A3) or the Epipaleolithic (C2, C3, C4, and C5) based on the presence or absence of pottery, while the remaining levels were without archeological remains.

Systematic excavation and reactivation of fieldwork took place in 1992 under the management of J. Bosch with others, expanding on Cantarell's trenches C and A (Fig. 2). Two sectors were defined: firstly, the Central Sector (an extension of the previous Sector A), which revealed the identification of five levels (1–5 Central).[1] Levels 2 and 4 were attributed to the Cardial Early Neolithic and Late Mesolithic, respectively (Level 3 was archaeologically sterile, and Level 1 was superficial). Secondly, the Inner Sector consisted of two overlapped levels (1/2-Interior) assigned to the Sauveterrian facies and Microlaminar Epipaleolithic, respectively (Fig. 3). Notable finds from this recent fieldwork include the productive association of a level belonging to the Sauveterrian technocomplex (1-Interior) and the identification of a level corresponding to the Geometric Mesolithic (4-Central) comprising a combustion structure, together with another one found in level 2-Central.

All this work has enabled a unified stratigraphic correlation (Bosch, 2005, 2016a). However, some of the associated levels show the possible formation of stratigraphic palimpsests due to the presence of incongruous materials. It should be emphasized that such palimpsests may be conditioned by episodes of variable intensity of water circulation within the cave (Bergadà, 1996). To address this, a detailed selection of contexts has been made, considering their relationship, the coherence of the artifacts they contain, and their chronological links based on the currently available dates (Table 1).

3. Material and methods

3.1. Sample, context selection and preservation of the assemblages

The analyzed assemblages represent 54.69 % (n = 1,002) of the total material recovered from all archaeological excavations. 751 artifacts associated with non-stratified surface areas (40.99 %) and 79 artifacts (4.32 %) from stratigraphic contexts considered unreliable (C1, C2, A1, B1, B2, EII, and EIII) have been excluded. The analyzed sub-assemblages attributed to each occupational phase are as follows:

[1] Level 5 in the Central Sector has a boundary defined by the significant reduction in the number of archaeological remains, with hardly any lithic artifacts (n=1) and little fauna, as no sedimentological change was detected in 1992. Due to these circumstances, it has not been included in the analysis and currently, the characterization and possible subdivision of Level 5 are under review.

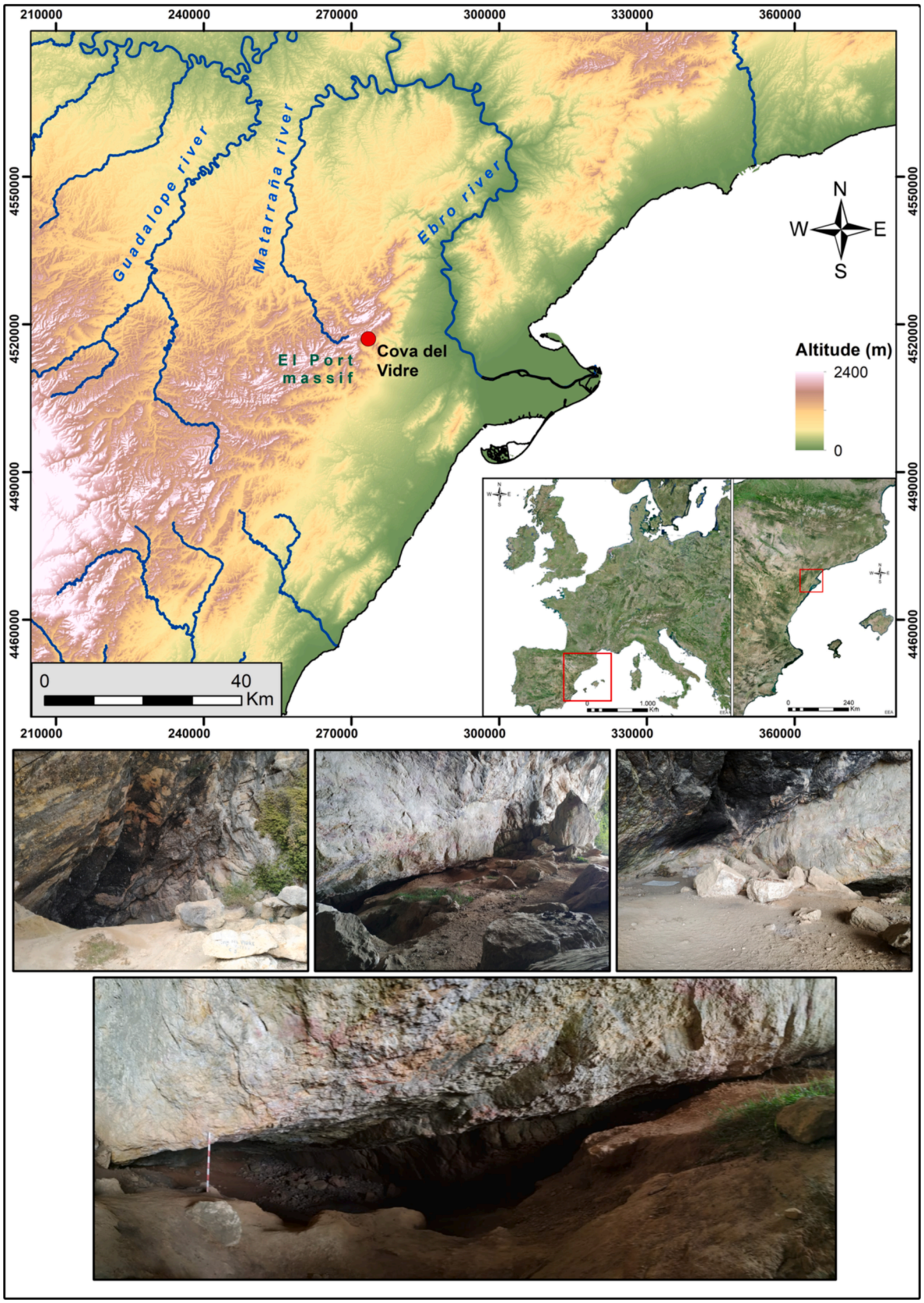

Fig. 1. Top: Digital Elevation Model showing the location of Cova del Vidre (topographic base: ICGC and EEA). Bottom (left to right): Main entrance; partial view of Central sector (1992); entrance to second small inner chamber adjoined to the north wall of the main chamber (Photographs: SAPPO-GRAMPO, 2019).

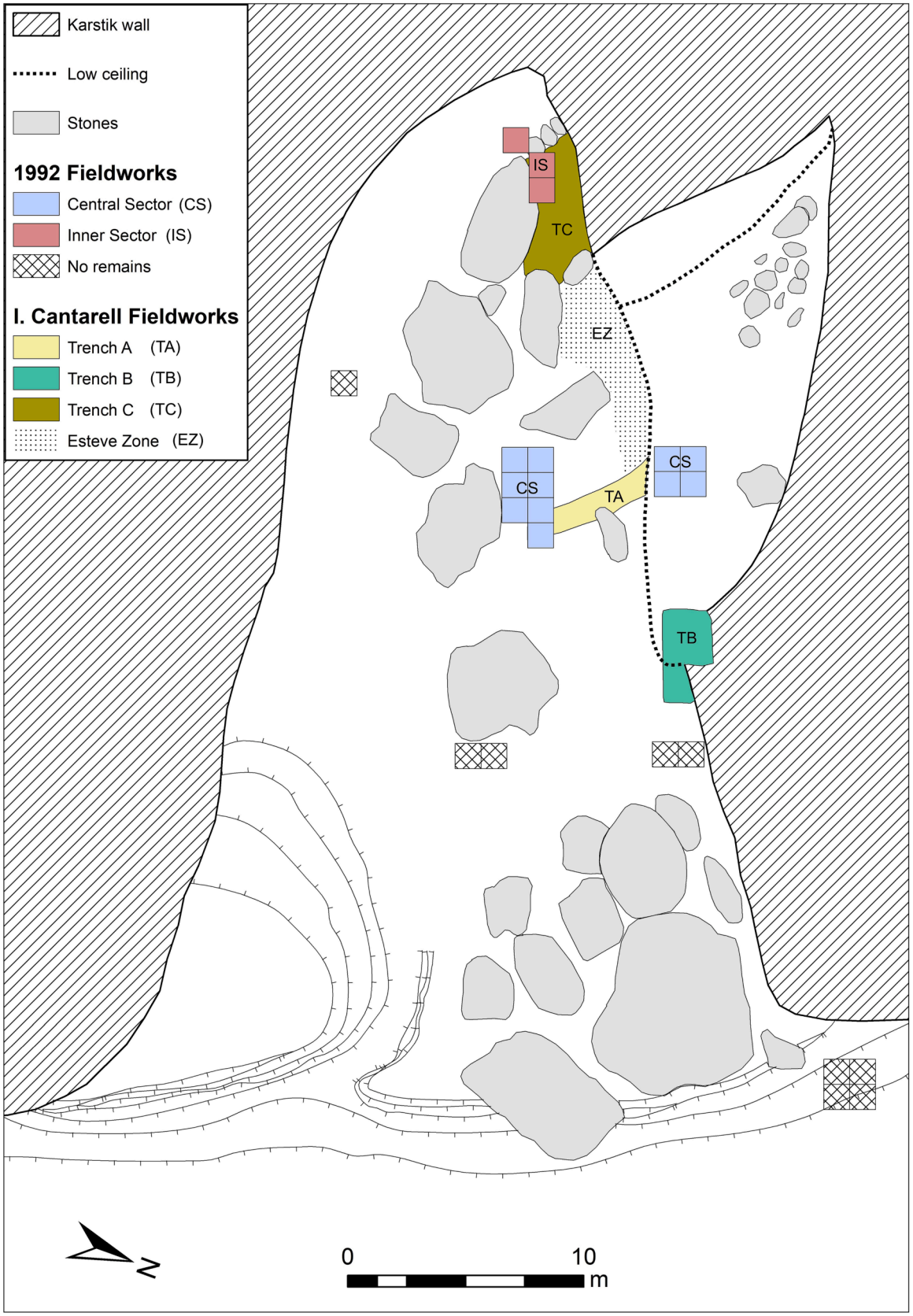

Fig. 2. Plan of Cova del Vidre and elevation with F. Esteve Gálvez, I. Cantarell and J. Bosch's excavation areas. Merger and digitalisation of original documents by I. Cantarell and J. Bosch (2005).

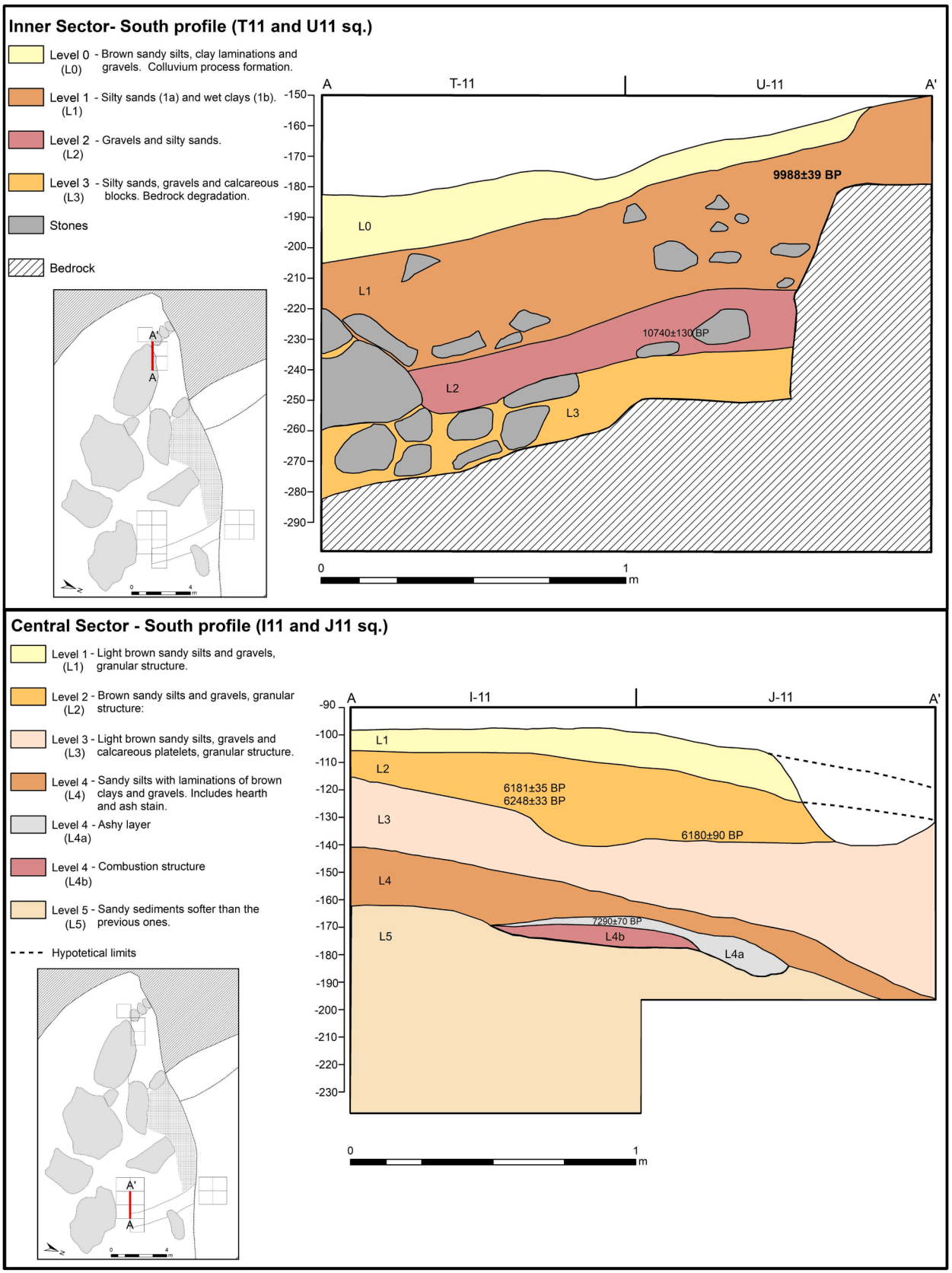

Fig. 3. Inner Sector and Central Sector section digitalisation from Bosch, 2005.

Table 1
Available absolute dates for levels documented in Cova del Vidre in 1992.

Layer	Lab_ID	Sample	Z (cm)	Square	BP	Cal. BC (2 s)	Cultural Ads.	Ref.
2-Interior	Beta 58,933	CH	−226	U11	10740 ± 130	11118-10521	Microlaminar Epipaleolithic	Bosch, 2005; 2016a
1-Interior	D-AMS 049,988	Bone	−180	U11	9988 ± 39	9740-9320	Sauveterrian	This work
4-Central	UBAR 832	CH	−167	I11	7290 ± 70	6361-6016	Late Mesolithic	Bosch, 2016a
2-Central	Beta 58,934	CH	−138	J11	6180 ± 90	5286-5003	Early Cardial Neolithic	Bosch, 2016a
2-Central	Ox A 26,064	Bone	−118	I11	6181 ± 35	5217-5007	Early Cardial Neolithic	Bosch, 2016a
2-Central	Ox A 26,065	Bone	−122	I11	6248 ± 33	5309-5071	Early Cardial Neolithic	Bosch, 2016a

- Microlaminar Epipaleolithic (ME): C5 and 2-Interior (n = 207)
- Sauveterrian (SAU): C3/C4 and 1-Interior (a/b) (n = 527)
- Late Mesolithic (LM): 4-Central (n = 133)
- Early Cardial Neolithic (ECN): A2 and 2-Central (n = 135)

In terms of preservation, all lithic artifacts in these assemblages (modified and unmodified, see Table 2) show similar proportions of complete elements (30–40 %), with slightly lower percentages in ECN assemblage. There is a predominance of long fragments (>50 % of the objects, 40–52 %) compared to short fragments.

Regarding blade industries, complete elements amount to less than 30 % in all cases. Proximal fragments dominate in all cases (between 28 and 33 %), except in ME assemblage, where medial fragments predominate (38 %). Finally, distal fragments account for around 20–25 %, with ECN assemblage having a lower proportion (13.33 %), and the remaining medial fragments showing roughly equal proportions between ME and SAU assemblages, with the lowest proportion in LM assemblage (13.51 %).

The fragmented elements of the assemblages correspond globally to 77.46 % for blade blanks and 68.3 % for flake blanks. Therefore, complete flakes account for 31.7 % and complete blades for 22.54 % of the assemblages.

Additionally, a series of thermal alterations have been identified on the analyzed artifacts, accounting for a high percentage relative to the total artifacts (40.21 %) (Table 3). For each assemblage, thermal alterations appear on 30.92 % of ME assemblage, 41.37 % of SAU assemblage, 32.33 % of LM assemblage, and 57.78 % of ECN assemblage. In these cases, alterations related to the optimization of the material predominate (75.18 %), and they do not affect the artifacts negatively. These alterations include thermal glosses, color changes, and thin, matte patinas on the objects. Some of these alterations show combinations of these effects. On the other hand, attributes such as flaking (or pot-lids), thermal bubbles, fissures and thermal fractures account for 24.82 % of the alterations, mostly combined with some type of non-aggressive alteration. All these thermal alterations may be indicative of the same patterns of space use, as recurrent combustion activities were detected in the last two phases of occupation, with the possibility of their presence in the preceding phases due to the abundant charcoal remains as indirect evidence (Alcolea et al., 2022).

3.2. Methodology

3.2.1. Bayesian chronological modelling

Chronological modelling was applied to refine the temporal definition of the lithic assemblages adding the new radiocarbon date. This allowed the integration of these dates into the complete sequence of the site through a continuous order sequence chronological model. This type of Bayesian model is the best approach to determine the duration of Cova del Vidre phases. The continuous order sequence chronological model assumes the existence of time intervals between the different phases, providing a more realistic and accurate chronology through Bayesian modelling. Using the gaps between the calibrated radiocarbon dates, it could calculate the duration of the stratigraphic interruptions or hiatuses: approximately 507 years between the two oldest levels, 2952 years between level 1-Interior and level 4-Central and 710 years between level 4-Central and level 2-Central, which includes the archaeologically barren level 3-Central.

3.2.2. Lithic analysis

The determination of raw materials has used macroscopic criteria through visual inspection and a stereo-microscope to categorize flint qualities following the proposal of X. Mangado (2004). Groups of raw material (MP) were characterized based on qualitative criteria: type of mineral, color, its combination (monochromatic/bichromatic/polychromatic), color distribution (homogeneous/irregular/banded/mottled), transparency (opaque, transparent, opaque with transparent edges), texture (fine, microcrystalline, aphanitic), luster (presence/absence), cortical (NC/<50 %/>50 %/C), and quality (low, medium, high; with mid-stage like medium–low and medium–high). These definitions were equally applied to the archaeological samples and the reference material from the lithotheque in the IMF-CSIC (Ortega et al., 2016). The archaeological samples were compared to the lithoteque material based on the

Table 2
Number and percentage of blanks and fragmented remains in each assemblage.

	ME			SAU			LM			ECN		
	N	%	% blanks	N	%	% blanks	N	%	% blanks	N	%	% blanks
FLAKES	**91**	**100.00**	**43.96**	**310**	**100.00**	**58.82**	**96**	**100.00**	**72.18**	**74**	**100.00**	**54.81**
Complete	28	30.77		98	31.61		37	38.54		18	24.32	
Short fragment	22	24.18		44	14.19		17	17.71		12	16.22	
Largue fragment	40	43.96		159	51.29		41	42.71		39	52.70	
Indet. (frag.)	1	1.10		9	2.90		1	1.04		5	6.76	
BLADES/BLADELETS	**115**	**100.00**	**55.56**	**205**	**100.00**	**38.90**	**37**	**100.00**	**27.82**	**60**	**100.00**	**44.44**
Complete	33	28.70		41	20.00		11	29.73		9	15.00	
Proximal	33	28.70		68	33.17		12	32.43		20	33.33	
Medial	25	21.74		44	21.46		5	13.51		23	38.33	
Distal	24	20.87		52	25.37		9	24.32		8	13.33	
CORES	**1**		**0.48**	**12**		**2.28**	**0**		**0.00**	**1**		**0.74**
TOTAL	**207**		**100**	**527**		**100**	**133**		**100**	**135**		**100**

Table 3
Number and percentage of thermal alterations in each assemblage. The category "combination" corresponds to the combination of two or more thermal alterations in the same artifact.

THERMAL ALTERATIONS		ME		SAU		LM		ECN	
		n	%	n	%	n	%	n	%
Thermal Optimum Alterations	Thermal Gloss (LT)	29	64.44	105	66.46	23	71.88	56	82.35
	Color Change (CC)	4	8.89	3	1.90	1	3.13	0	0.00
	Thermal Patina (PT)	0	0.00	0	0.00	0	0.00	0	0.00
	Combinations (>1)	12	26.67	50	31.65	8	25.00	12	17.65
	TOTAL	**45**	**100**	**158**	**100**	**32**	**100**	**68**	**100**
Overheated Alterations	Cracked/Scale fissures (Cq)	0	0.00	3	5.00	1	9.09	0	0.00
	Thermal bubble (CT)	0	0.00	4	6.67	0	0.00	0	0.00
	Thermal Pot-lid flake (ET)	0	0.00	1	1.67	0	0.00	0	0.00
	Thermal Fracture (FT)	0	0.00	0	0.00	0	0.00	0	0.00
	Combinations (>1)	19	100	52	86.67	10	90.91	10	100
	TOTAL	**19**	**100**	**60**	**100**	**11**	**100**	**10**	**100**
Sum thermal alterations		**64**	**30.92**	**218**	**41.37**	**43**	**32.33**	**78**	**57.78**
Total analysed		**207**		**527**		**133**		**135**	

defined groups of raw material and associated with their corresponding geological formations of origin (G) at a regional scale. This provided a preliminary identification of the possible procurement radii of raw materials from primary outcrops based on current geological data (ICGC).

For the lithic technological analysis, the definition of typometric blanks (flake and blade) according to Brézillon (1977) was adopted. Within laminar blanks, bladelets were defined based on the width cutoff value (<12 mm) provided by Tixier (1963). The length value was omitted due to the high proportion of fracture in the assemblages, all oriented along their percussion axis.

The cores were classified under García-Puchol criteria (2005), specifying the morphology and adding bipiramidal category, the number of extraction planes, the direction of extractions (Unipolar/Bipolar/Centripetal/Multiple), and the percussion surface (flat/prepared) (García-Puchol, 2005) were registered. Additionally, the type of knapped blanks and their count (Flake/Blade/Bladelet), the condition of the striking platform (Irregular/Partial abrasion/Total abrasion), the extent of exploitation (Irregular/Enveloping/Semi-Enveloping/Unifacial/Bifacial opposite), identifiable knapping errors (Reflex/Fracture/Overshot), and the presence of macroscopically visible use-wear traces were also noted. Cores were measured based on their knapping orientation depending on their morphology: oriented parallel to their percussion axes (unipolar, bipolar and centripetal) or based on their maximum and minimum dimensions in case they are not morphologically identifiable, and for globular cores.

Due to the limited presence of cores in the assemblage, a brief classification of products with technological attributes was added, providing information about the implemented production strategies. We used Fortea (1973) and Juan-Cabanilles (2008) criteria for typometrics, typology, and retouching. This criterion uses a hierarchical type list and its breakdown into sub-types, defined by technological and morphological aspects. The definition of retouching was simplified by selecting variables such as inclination, facial extension, direction, general delineation, and special delineation (Juan-Cabanilles, 2008:25). In every retouched group we have specified its location according to the percussion axis of the object concerning the dorsal face.

Statistical tests were applied to metric variables to compare the length and width of flakes and blades between assemblages (See discussion section). These tests include normality tests (<50 samples, Shapiro-Wilk; >50 samples, Kolmogorov-Smirnov/Lilliefors) (Shapiro and Wilk, 1965; Lilliefors, 1967), parametric tests (Bartlett Test. Bartlett, 1937), or non-parametric tests (Kruskal-Wallis. Kruskal & Wallis, 1952) to explore differences in metric values based on the acceptance or rejection of the null hypothesis (H_0). When the null hypothesis was rejected in the non-parametric tests, Post-hoc tests (Dunn's Test, p. adj. Bonferroni. Dunn, 1964) were performed to identify, when applicable, variability among the assemblages as Alternative Hypothesis (H_1). Simple Linear Regressions (Kenney & Keeping, 1962) were applied for length and width complete flakes values, after checking their residuals using normality tests (Shapiro-Wilk) and homoscedasticity tests (Breusch-Pagan Test. Breusch & Pagan, 1979).

The statistical tests and associated graph figures were carried out on R software (R Core Team, 2018), using the *rstatix*, *broom*, and *ggplot2* packages.

Code and data related to this work are available in Zenodo repository (https://doi.org/10.5281/zenodo.10161086, Gironès et al., 2023).

4. Results

4.1. Chronological sequence of Cova del Vidre

The radiocarbon date obtained has been subjected to Bayesian modelling with the others published previously. The new date was carried out on a bone sample from the interior level 1 in 1992, specifically on the distal diaphysis of a *Capra pyrenaica* femur. It was sent to the DirectAMS laboratory (WA, USA) for radiometric analysis and to the Stable Isotopes Ecology laboratory (University of Georgia, USA) for isotope analysis. To model the sequential order of the radiocarbon dates according to the phases recorded in the two excavations, OxCal software version 4.4.4 (Bronk-Ramsey, 2021) was used, with the IntCal20 calibration curve (Reimer et al., 2020) and the application of a model of sequences with contiguous order based on the radiocarbon dates and their relationship with the superposition of associated levels (Fig. 4).

Therefore, the order of the data used has been maintained according to the clear superposition of the stratigraphic levels and the coherence of the archaeological remains associated with each level. The results of the modeling have provided high correlation indices, exceeding 60 % (Aoverall = 100.8), as well as the overall consistency of the model (Amodel = 99.9). These results imply that the construction of the Bayesian model is robust and reliable, thus making the outcomes statistically valid. In this case, the duration of the sequential assemblage is 6259 years (1 sigma) or 7622 years (2 sigmas) (Table 4), comprising an initial phase from the late 11th millennium cal. BC, corresponding to the Microlaminar Epipaleolithic. Although the available date has a high standard deviation (±130), it may display continuity with the later occupation, which covers a range from the late 11th millennium to the middle 9th millennium cal. BC. Generally, within this overall range, there are certain temporal gaps: between levels 1-Interior and 4-Central, and another one between the latter and 2-Central, as observed in the mentioned stratigraphic traits. It is worth noting the inclusion of the Late Mesolithic in the model, although its subphase is indeterminate (7184–5646 cal. BC, 1 sigma), as well as the continuity of dates

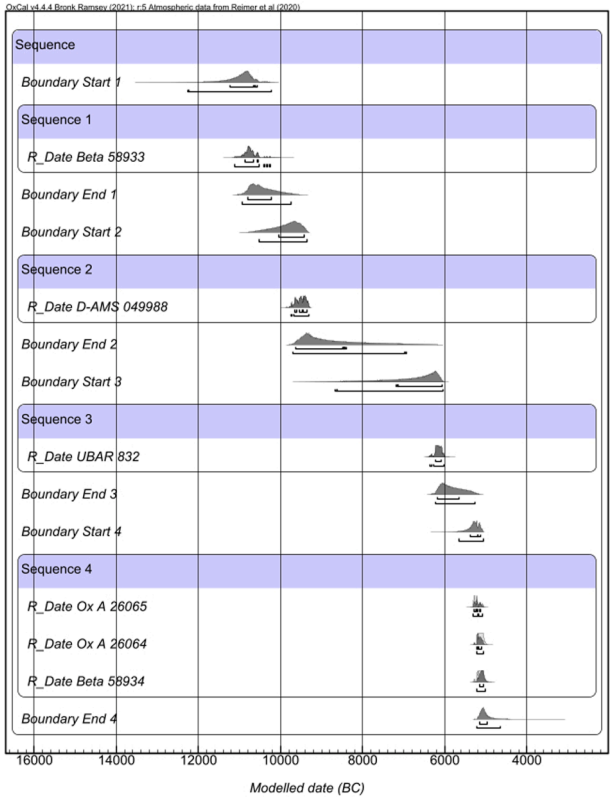

Fig. 4. Bayesian phase chronological model multiplot with available 14C data.

corresponding to the Early Cardial Neolithic without any internal hiatus (5376–4971 cal. BC, 1 sigma).

4.2. Lithic analysis

4.2.1. Raw material

The lithic assemblages from Cova del Vidre are heterogeneous in terms of siliceous rocks and quality (Table 5). The macroscopic analysis was applied to 1,002 lithic artifacts from the four assemblages. We have identified 16 siliceous groupings of different qualities (see Table 1a supplementary material), including low-quality chert (MP9, MP11, and MP15), and the predominance of flint in 13 distinct groupings (99.1 %). Unidentified flint due to patina or thermal alterations is included as a unified category (25.14 %) (see Table 1b supplementary material).

Within the flint groupings, lacustrine carbonated materials (MP2 and MP13) stand out and are predominant in ME and SAU assemblages. In contrast, lacustrine evaporitic materials (MP4, MP5, MP15, and MP10) appear in equal proportions in the more recent assemblage.

The acquisition of these materials corresponds to the formations detected in the nearby territory (Rey-Solé et al., 2015; Ortega et al., 2016) (Fig. 5). On one hand, the lacustrine carbonate formations originating in the Ebro Depression are strongly represented (G2), with primary outcrops located around 25–50 km or even up to 100 km away (Fm. La Fatarella and Fm. Torrent del Cinca, respectively). These materials could also have been obtained from secondary outcrops near the main waterways based on the evidence of cortical rolling (Table 6). On the other hand, there is a lower quality trend but heterogeneity in the attributes of materials from different evaporitic formations throughout the Catalánides and their connection with the Iberian System. Some comparative similarities between materials can be observed (G3-G6 Fm. Valldeperes/Ud. Vilaverd; G4 Ud. Horta de Sant Joan/Fm. Ulldemolins or Ud. Font de la Salut), with radii ranging from 25 to 50 km and

Table 4
Results from the Bayesian phase chronological model.

	Sequence	BP	Unmodelled (2 s)		Modelled				Bound. range (Cal. BC, 1 s)	Bound. range (Cal. BC, 2 s)	$\delta^{13}C$ (‰)	$\delta^{15}N$ (‰)	C/N
			from	to	from	to (1 s)	from	to (2 s)					
Sequence 1	Boundary Start 1				**−11230**	**−10581**	**−12269**	**−10223**	11230–10230	12269–9747			
	R_Date Beta 58,933	10740 ± 130	−11118	−10521	−10876	−10553	−11115	−10246					
	Boundary End 1				**−10807**	**−10230**	**−10925**	**−9747**					
Sequence 2	Boundary Start 2				**−10039**	**−9434**	**−10528**	**−9365**	10039–8409	10528–6943	−19.78	2.76	3.31
	R_Date D-AMS 049,988	9988 ± 39	−9740	−9320	−9656	−9366	−9739	−9318					
	Boundary End 2				**−9634**	**−8409**	**−9708**	**−6943**					
Sequence 3	Boundary Start 3				**−7184**	**−6077**	**−8677**	**−6034**	7184–5646	8677–5277			
	R_Date UBAR 832	7290 ± 70	−6361	−6016	−6224	−6079	−6366	−6016					
	Boundary End 3				**−6180**	**−5646**	**−6226**	**−5277**					
Sequence 4	Boundary Start 4				**−5376**	**−5126**	**−5658**	**−5071**	5376–4971	5658–4647			
	R_Date Ox A 26,065	6248 ± 33	−5309	−5071	−5298	−5130	−5306	−5081					
	R_Date Ox A 26,064	6181 ± 35	−5217	−5007	−5214	−5106	−5218	−5060					
	R_Date Beta 58,934	6180 ± 90	−5286	−5003	−5155	−5052	−5211	−5021					
	Boundary End 4				**−5161**	**−4971**	**−5215**	**−4647**					

Table 5
Number and proportion of the total raw material groups identified and unidentified in each assemblage: MP = raw material quality groups; G = outcrops group as geological formation.

GROUP	MP (Quality groups)	ME		SAU		LM		ECN	
Flint		*n*	*%*	*n*	*%*	*n*	*%*	*n*	*%*
G1	MP1; MP6	1	0.48	0	0.00	0	0.00	12	8.89
G2	MP2, MP13	44	21.26	243	46.11	79	59.40	37	27.41
G3	MP3, MP5, MP8, MP12	8	3.86	76	14.42	39	29.32	39	28.89
G4	MP4, MP14	35	16.91	45	8.54	9	6.77	6	4.44
G5	MP10	0	0.00	5	0.95	0	0.00	2	1.48
G6	MP7	1	0.48	1	0.19	0	0.00	1	0.74
G7	MP16, MP6T	27	13.04	31	5.88	0	0.00	0	0.00
		116	56.04	401	76.09	127	95.49	97	71.85
Chert									
G9	MP9,MP11,MP15,MP17	1	0.48	6	1.14	0	0.00	2	1.48
Thermal Alterations + Indet.									
G10	MP1T,MP5T,MP7T	2		9		3		11	
G11	MP2T	0		0		0		2	
G12	MP4T	0		1		0		0	
G13	MP3T	2		1		0		6	
G0	MP0	86		109		3		17	
G. Indet		90	43.48	120	22.77	6	4.51	36	26.67
	TOTAL	**207**	**100.00**	**527**	**100.00**	**133**	**100.00**	**135**	**100.00**

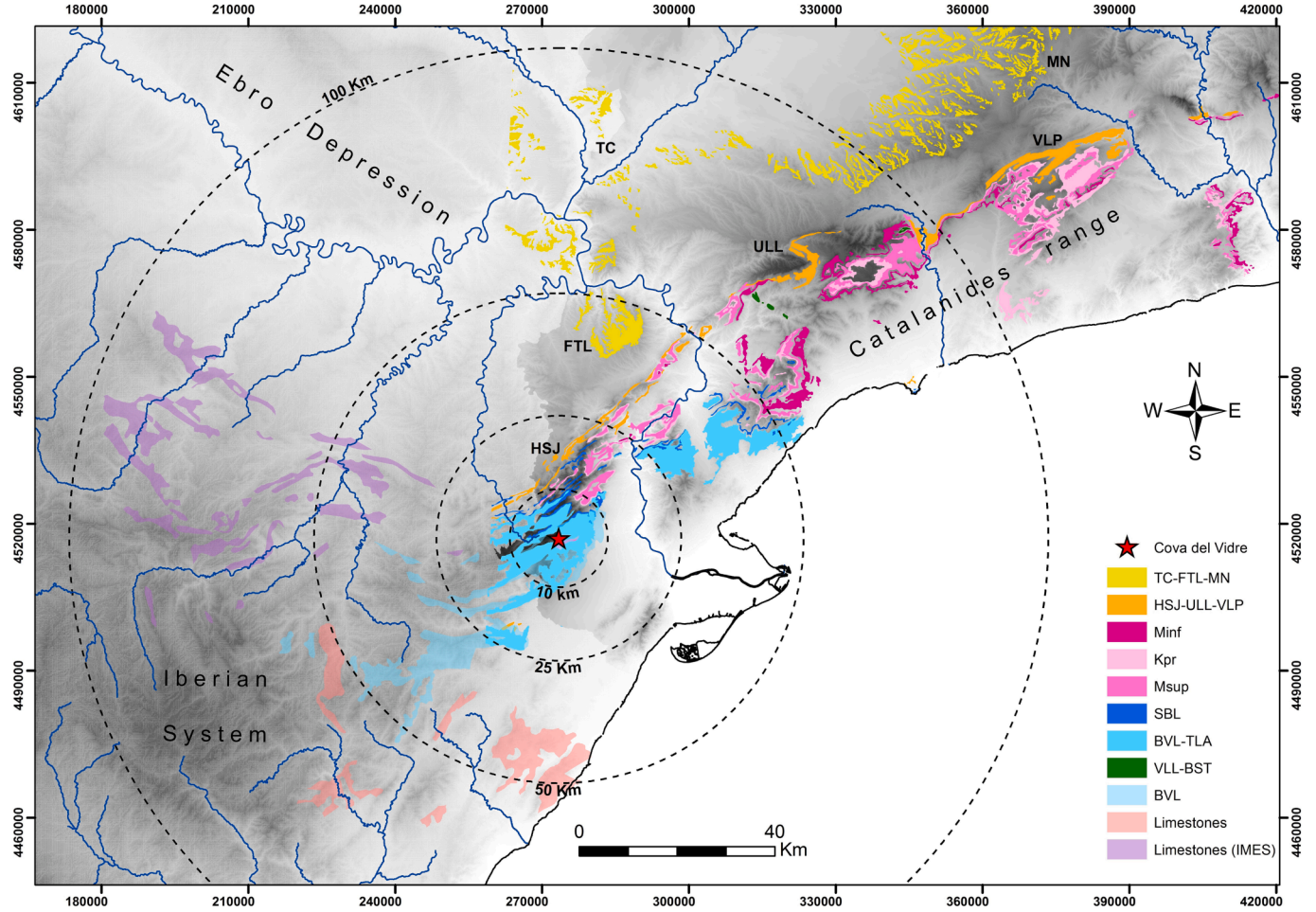

Fig. 5. Regional geological map with carbonated lacustrine flint primary outcrops (TC-FTL-MN, yellow) and the different geological formations of evaporitic lacustrine primary outcrops and optimal limestone formations near Cova del Vidre: Fm. Torrent de Cinca – Fm. Fatarella-Fm. Montmaneu (TC-FTL-MN); Ud. Horta de Sant Joan - Cm. Ulldemolins - Fm.Valldeperes (HSJ-ULL-VLP); Fm. Sant Blai (SBL); Fm. Bovalar and Talaies (BVL-TAL); Fm. Vilelles and Bassetes (VLL-BST); Fm Miravet, Molar and Gallicant (Kpr); Fm Brull, Olesa and Vilella Baixa (Minf); Fm. Colldejou and Benifallet (Msup). Topographic base: ICGC; Database modified from ICGC; data location extracted from Ortega et al., 2016. (For interpretation of the references to color in this figure legend, the reader is referred to the web version of this article.)

Table 6
Distribution of cortex and rolled cortex according to raw material quality groups (MP) and outcrop association groups (G) for each assemblage (Ctx. = Total Cortical pieces; Rd. Ctx. = Rolled cortical pieces).

Raw material groups	Raw material quality groups	ME			SAU			LM			ECN		
		n (Ctx.)	n (Rd. Ctx.)	% (Rd. Ctx.)	n (Ctx.)	n (Rd. Ctx.)	% (Rd. Ctx.)	n (Ctx.)	n (Rd. Ctx.)	% (Rd. Ctx.)	n (Ctx.)	n (Rd. Ctx.)	% (Rd. Ctx.)
G1	MP1; MP6	0	0	0	0	0	0	0	0	0	2	0	0
G2	MP2, MP13	13	9	69.23	73	57	78.08	27	16	59.26	11	4	36.36
G3	MP3, MP5, MP8, MP12	1	1	100	16	11	68.8	11	6	54.55	1	0	0
G4	MP4, MP14	8	6	75	17	9	52.94	1	0	0	2	0	0
G5	MP10	0	0	0	1	0	0	0	0	0	0	0	0
G6	MP7	0	0	0	0	0	0	0	0	0	0	0	0
G7	MP16,MP6T	9	7	77.78	8	5	62.5	0	0	0	0	0	0
TOTAL		**31**	**23**		**115**	**82**		**39**	**22**		**16**	**4**	

secondary outcrops at shorter distances (G3 and G4). Formations such as Fm. Sant Blai (G5) and Fm. Bovalar-Talaies lie within entirely local radii (<10 km). One material group (G1) remains unidentified in terms of its origin; characterized by high-quality blonde flint not attributable, now, to the Bedoulian flint (Molist et al., 2016), it might possibly be considered an exogenous material (>100 km). Additionally, G7 is an undetermined evaporitic material, which could be obtained locally or supraregionally and exhibits a high proportion of rolled cortex.

4.2.2. *Technology*

4.2.2.1. Microlaminar Epipaleolithic technology. The Microlaminar Epipaleolithic assemblage entails a predominance of laminar reduction (over 55 %, Table 2: ME assemblage) and a significant microlaminar index (48.45 %), the latter primarily falling within the 8–10 mm width range (Fig. 6: ME assemblage). The metric data for width, excluding modified pieces (backed pieces, burins, and perforators that involve complete uni/bilateral modifications) is established by mean width values of 12.85 ± 5.37 mm (n = 97, see Table 3 supplementary material: ME assemblage). In addition, 22 complete products (22.68 %) are identified, with mean measurements of 38.40 mm in length, 14.63 mm in width, and 6 mm in thickness (see Table 2 supplementary material: ME assemblage).

On the other hand, we identified the raw material quality groups for 49 laminar blanks (Fig. 7: ME assemblage; see Table 4 supplementary material: ME assemblage), which samples larger than 10 objects show lower means for MP2 (12.07 ± 5.04 mm), followed by MP4 (13.37 ± 5.15 mm) and MP16 (14.93 ± 7.36 mm). The other material quality groups among the blades are scarcely represented (MP9, MP5, MP12 and MP13).

In contrast, the flakes account for less than 50 % of blanks and are associated with mean lengths of complete pieces of 28.44 ± 12.93 mm and 21.62 ± 10.17 mm width. For the fragmented pieces are less, characterized by mean lengths of 18.9 ± 7.12 and mean widths of 16.8 ± 6.7 (Fig. 8: ME assemblage).

Any direct evidence of elements associated with this type of production are observed, except for a single example consistent with laminar reduction (Fig. 9: ME assemblage). This is represented by

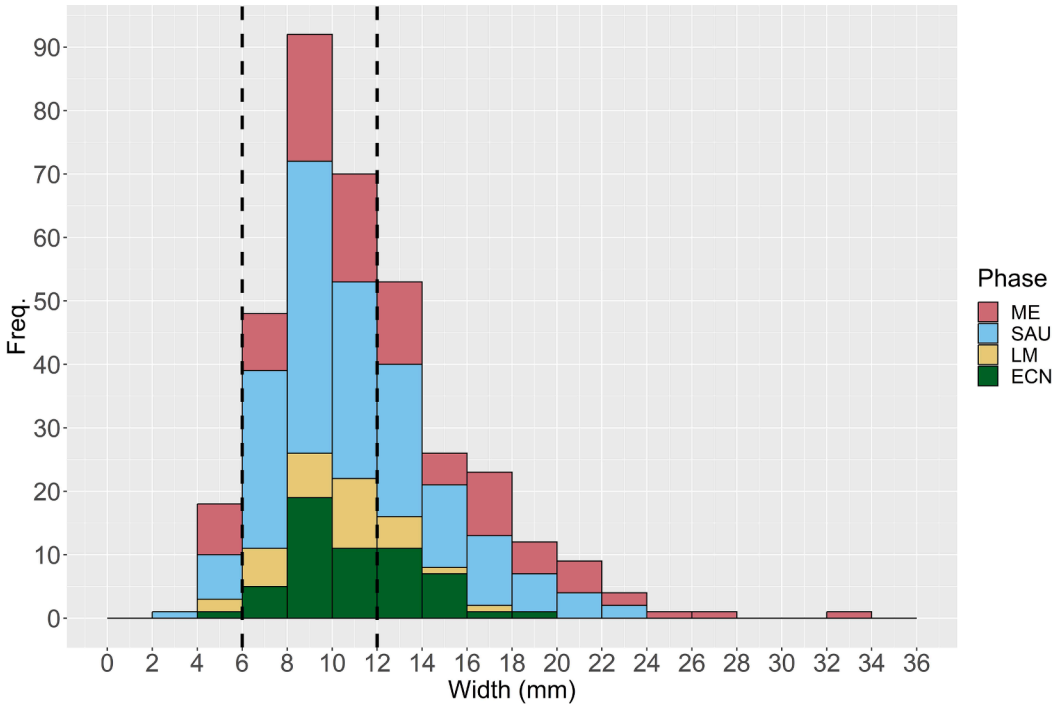

Fig. 6. Stacked bar plot of absolute frequency of blades width values. The metric criteria defining microblade blanks (from different authors) are marked with a dashed line.

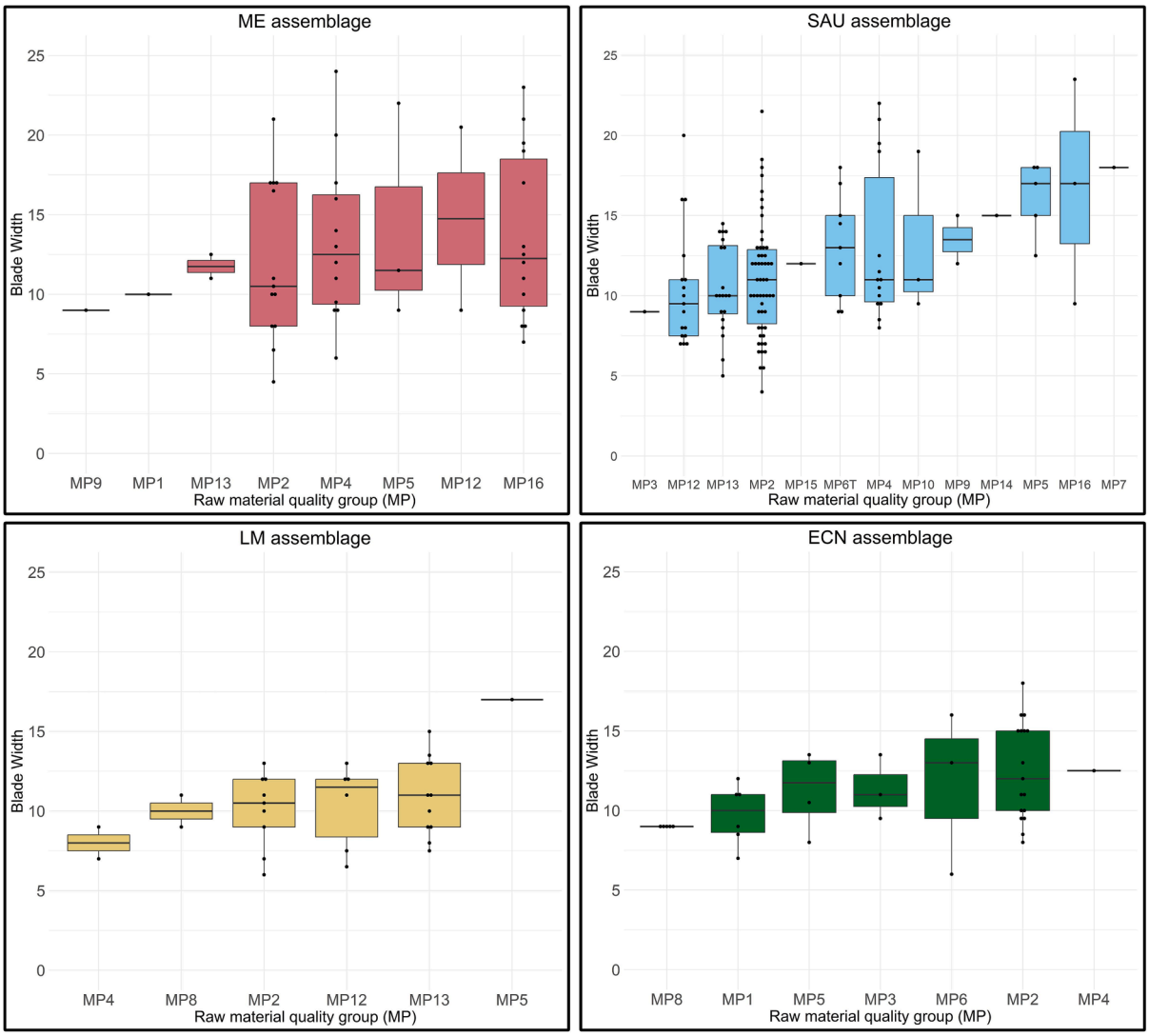

Fig. 7. Boxplots showing blade width related to raw material quality groups identified in each assemblage.

bidirectional prismatic core (36.5 × 19 × 15.5 mm) with partial blade and microblade production, featuring morphological reconfigurations through flaking, including a partial lateral crest, where both platforms are flat.

Due to the lack of a consistent sample of cores, the categorization and counting of objects with technological features (Table 7: ME assemblage) indicate items associated with laminar cores. It includes laminar flakes (30.77 %), some modified through retouch (n = 7), and the presence of ridges on laminar blanks (n = 5) and on flakes (n = 1).

The decortication evidence of the core is present according to 7 entirely cortical pieces (dorsal surfaces), mostly laminar (only one flake), belonging to materials MP3T, MP2, and MP16 (n = 2) and with the remaining three on unidentified flint (MP0).

4.2.2.2. Sauveterrian technology. The Sauveterrian assemblage is characterized by a predominance of flaking (58.82 %, Table 2: SAU assemblage), with average lengths of 19.2 ± 8.9 mm and widths of 15.9 ± 6.1 mm for complete items. For fragmented pieces, the lengths have an average of 19.96 ± 8.21 mm and widths of 17.01 ± 6.98 mm (Fig. 8: SAU assemblage).

Laminar production accounts for less than 39 % (n = 205) in this case, characterized by blades with an average width of 11.54 ± 3.95 mm (excluding previous morphotypes, n = 173, see Table 3 supplementary material: SAU assemblage) and a high presence of bladelets (58.95 %), with the highest metric concentration between 10 and 12 mm in width (Fig. 6: SAU assemblage). Complete laminar pieces represent 17.34 %, with average lengths of 31.10 mm, widths of 12.28 mm, and thicknesses of 5.31 mm (see Table 2 supplementary material: SAU assemblage).

Within the total blades, the raw material quality groups have been identified in 131 objects (Fig. 7: SAU assemblage). Groupings on these objects allow observing the predominance of MP2 remains consistent with microblade standards (11 ± 3.59 mm), as well as MP13 (10.47 ± 2.8 mm) and MP12 (10.44 ± 3.75 mm), but not MP4 (13.1 ± 4.95 mm) and MP6T (13.05 ± 3.33 mm), and MP5 (16.1 ± 2.35 mm) with low representation (see Table 4 supplementary material: SAU assemblage).

The direct presence of cores accounts for 2.28 % of the supports in the assemblage, and all material groups associated with them have been identified (Fig. 9: SAU assemblage). Three different morphologies have been defined: globular cores (n = 4) with enveloping flaking exploitation and very small sizes (MP2, MP4 and MP5), including one core with bladelet and flake production reutilized as a percussion tool (MP13). Pyramid cores (n = 2), one bidirectional (MP13) and one unidirectional (MP2), correspond to blade and microblade enveloping debitage with similar sizes. Discoid cores (n = 4) are characterized by three centripetal (two MP2 and one MP4) and one bidirectional configuration (MP2), three of them with microblade extractions with enveloping or semi-enveloping exploitation. The last discoid centripetal core was employed in flaking production. Finally, one core with irregular

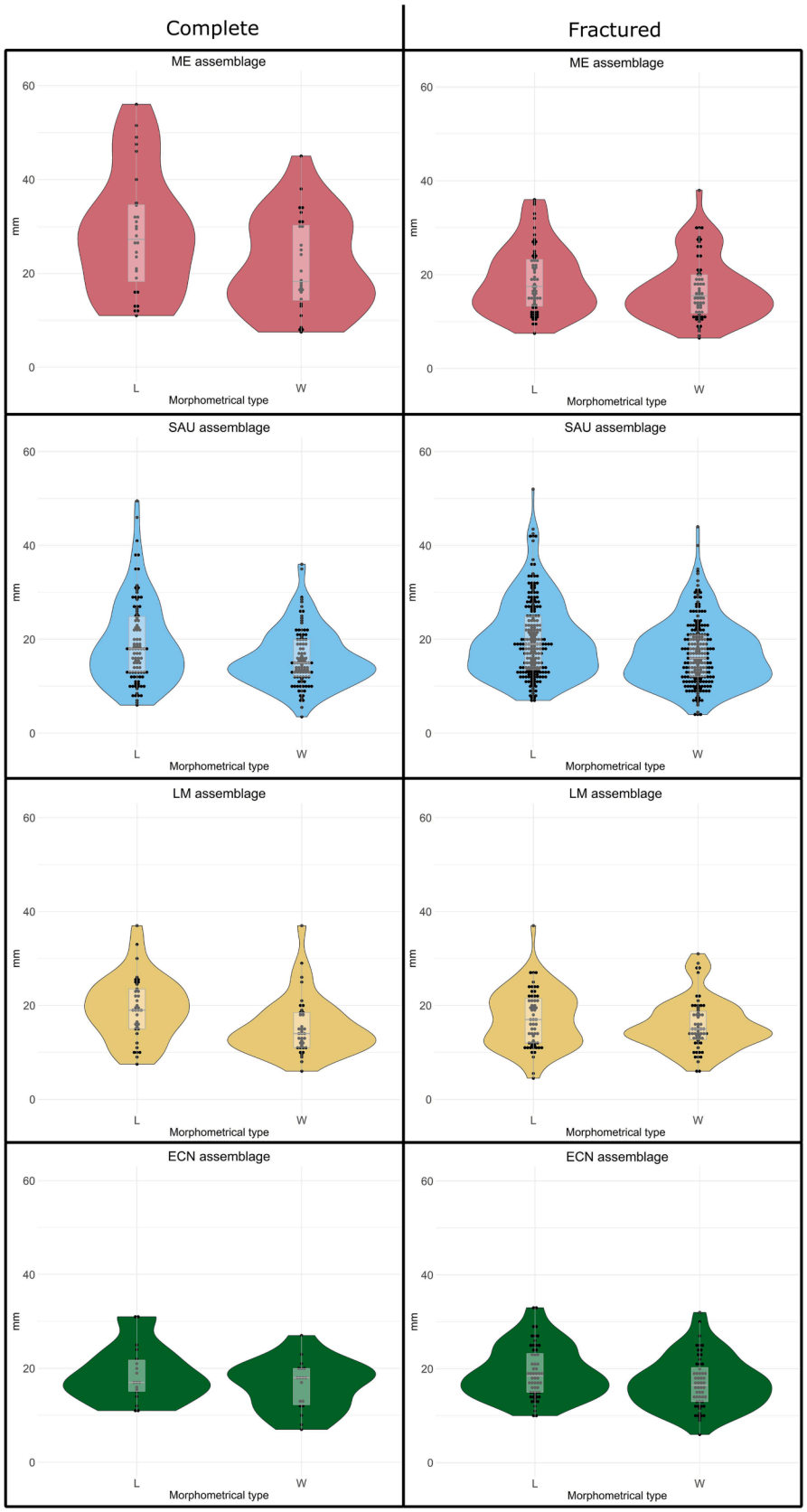

Fig. 8. Violin plots of Length (L) and Width (W) values of complete/fragmented flakes in each assemblage. It shows the Kernel probability distribution: wider sections represent a higher probability and skinnier sections have a lower probability on Length and Width values. It has added in grey the boxplot for each violin plot.

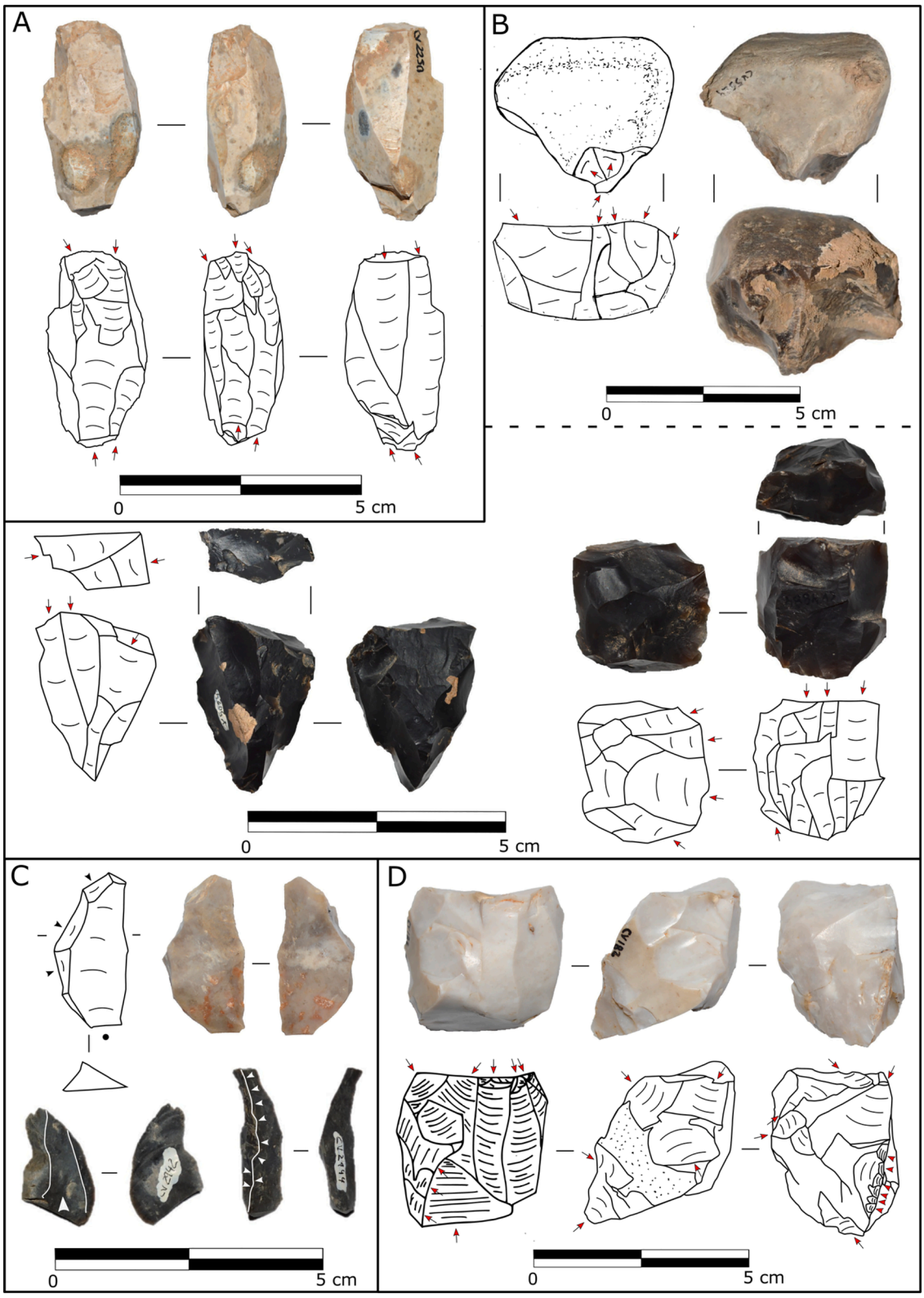

Fig. 9. Cores and indirect technological attributes defining knapping strategies identified in each assemblage ME (A), SAU (B), LM (C) and ECN (D): Prismatic bidirectional core with blade and microblade production (A); Core preform of G2 material with rolled cortex (B top); Pyramidal core with unidirectional blade production with prepared platform (B bottom-left); Globular core in configuration process: unfaceted with unidirectional microblade extraction and unifacetted flake extractions in opposite surfaces, enveloped exploitation (B bottom-right); Reconfiguration tablet (knapping platform), lamellar flake and crested blade (C); Core with in-process configuration pyramidal morphology, unidirectional blade production with smooth platform and partial lateral crest (D). Drawing by J. Bosch and I. Gironès.

Table 7
Number and percentage blanks with technological traits in each assemblage.

Blanks	ME		SAU		LM		ECN	
	n	%	*n*	%	*n*	%	*n*	%
Flakes	**91**	**44.17**	**310**	**60.19**	**96**	**72.18**	**74**	**55.22**
Primary Flakes	59	64.84	232	74.84	68	70.83	62	83.78
Crested Flakes	1	1.10	1	0.32	0	0	0	0
Lamellar Flakes	28	30.77	61	19.68	16	16.67	7	9.46
Cortical Flakes	3	3.30	14	4.52	10	10.42	5	6.76
Core tablets	0	0	1	0.32	1	1.04	0	0
Burin spalls	0	0	0	0	1	1.04	0	0
Thermal Pot-lid (flake)	0	0	1	0.32	0	0	0	0
Blades/Bladelets	**115**	**55.83**	**205**	**39.81**	**37**	**27.82**	**60**	**44.78**
Primary blades	106	92.17	168	81.95	28	75.68	55	91.67
Crested blades	5	4.35	12	5.85	3	8.11	1	1.67
Cortical blades	4	3.48	5	2.44	0	0	3	5
Burin spalls	0	0	2	0.98	0	0	0	0
Overshot blades	0	0	1	0.49	0	0	0	0
Microburins	0	0	17	8.29	6	16.22	1	1.67
TOTAL	**206**	**100**	**515**	**100**	**133**	**100**	**134**	**100**

morphology and unknown configuration (MP2), probably linked to an earlier stage of core shaping, only shows negatives of two products (a flake and a blade). The measurements of these cores indicate reduction and amortization to a small size: averages of 28.7 ± 5.23 mm (length) and 24.5 ± 5.4 mm (width), often due to knapping errors associated with the multiple technical actions (core fractures, hinge marks, platform angles greater than 90°). Platform preparation is present in four of these cores: a bidirectional core has one prepared platform and one flat platform, another globular core has one flat platform, and the remaining cores lack platform preparation, including one core without platform, directly cortical in the process of shaping.

These productions complement some technological features (Table 7: SAU assemblage). The presence of crests, predominantly on blades (n = 12), most of them are maintained on the established microlaminar metric (n = 10) without any modification through retouching. In addition to the laminar production, there is a notable presence of bladelets (19.68 %), some retouched (n = 19).

Cortical pieces are present for both types of supports, both in blades (n = 14) and on bladelets (n = 4), with predominantly microlaminar attributes within the latter (n = 3). The identified material groups correspond to MP2 (n = 2), MP13 (n = 5), MP14 (n = 1), MP5T (n = 1), and MP6T (n = 1), while the rest are unidentified. Additionally, a piece of core tablet rejuvenation is documented.

The microburins (n = 17) indicate the presence of geometric production, two of which belong to trihedral points, made on proximal (n = 7), medial (n = 4), and distal (n = 6) parts, predominantly on microlaminar supports (n = 14), and on identified materials belonging to MP2 (n = 6), MP12 (n = 1), MP13 (n = 3), MP4 (n = 1), and MP10 (n = 1).

Other types of knapping waste have been detected in three pieces, including the burin spalls defined by two small and thin bladelet. Technologically, there is also a completely overshot blade that includes partially the lower part of the blade production core at its distal end. Whatever the cause (accidental or technological), there is a thermal pot-lid (flake) detachment due to thermal overshot.

4.2.2.3. Late Mesolithic technology. The Late Mesolithic assemblage is characterized by flake production (72.18 %, Table 2: LM assemblage), with complete pieces averaging 19.36 ± 6.7 mm in length and 15.41 ± 6.23 mm in width. In the case of fragmented elements, lengths tend to average 17.11 ± 6.13 mm, and widths 15.77 ± 5.48 mm (Fig. 8: LM assemblage).

Laminar production is lower (27.82 %, n = 37), with an average width of 11.33 ± 2.98 mm (n = 33, see Table 3 supplementary material: LM assemblage), denoting a high proportion of bladelets (66.66 %) mostly ranging between 8 and 10 mm in width (Fig. 6: LM assemblage). Some blades are preserved complete (27.02 %) with average lengths of 24.55 mm, widths of 10.35 mm, and thickness of 4.15 mm (see Table 2 supplementary material: LM assemblage). Within all laminar blanks, raw material quality has identified 31 elements with metric values that tend towards microlaminar productions (Fig. 7: LM assemblage). It can be observed in MP13 (10.9 ± 2.45 mm), MP2 (10.05 ± 2.35 mm), and MP12 (10.33 ± 2.6 mm), with the remaining materials being less significant (see Table 4 supplementary material: LM assemblage).

In this assemblage, there is a complete absence of cores. To compensate, we observe certain technological features that evoke generic flint-knapping strategies (Table 7 and Fig. 9: LM assemblage). Among these, elements belonging to blade production stand out, such as blade flakes (n = 16), a few modified with retouch (n = 3) and belonging to MP2 (n = 5), MP4 (n = 2), MP12 (n = 4), and MP13 (n = 5). Additionally, crests on blades (MP2 and MP13) add more information about this type of knapping strategy.

Remains of tool configurations are present, although they are scarce. These include cortical pieces indicating core preparation, all on blades and belonging to different material groups (MP2, MP5, MP12, and MP13), a core tablet, and a burin spall remnant.

It is worth noting the presence of the microburin technique, with six total pieces, two of which belong to tridirectional points. All of them were divided into proximal (n = 4), medial, and distal parts (n = 1 each), metrically in line with microlaminar pieces (n = 3) and on materials MP2 (n = 2), MP12 (n = 1), and MP13 (n = 3).

4.2.2.4. Early Cardial Neolithic technology. The assemblage from the most recent phase maintains a slight predominance of flake production (54.81 %, Table 2: ECN assemblage) with mean lengths of 18.8 ± 6 mm and widths of 16.38 ± 5.35 mm for complete pieces, and 19.25 ± 5.61 mm in length and 16.97 ± 5.52 mm in width for fragmented pieces (Fig. 8: ECN assemblage).

In this context, blade production is notable (44.44 %) with 60 artifacts and mean widths of 10.37 ± 2.67 mm, excluding those previously excluded due to edge modification (n = 56, see Table 3 supplementary material: ECN assemblage). Microlaminar production gains importance within the total blade assemblage (58.92 %), predominantly ranging between 8 and 10 mm in width (Fig. 6: ECN assemblage).

The preservation of complete blade pieces is scarce (10.76 %), with mean lengths of 28.58 mm, widths of 10.16 mm, and thicknesses of 3.08 mm (see Table 2 supplementary material: ECN assemblage).

The raw material has been identified for 39 blade artifacts (see Table 4 supplementary material: ECN assemblage). The largest sample corresponds to MP2 with a mean of 12.5 ± 1.89 mm, scarce samples for MP5 (11.25 ± 2.53 mm) and exclusively microblade products such as

MP1 (9.75 ± 1.89 mm) and MP8 (9 ± 0 mm), while the remaining materials are less represented.

Only one core has been identified in this assemblage (Fig. 9: ECN assemblage) defined by a globular core (33 x 36 x 29 mm) with flake extractions for morphological reconditioning and unifacial blade production with a flat platform.

The remaining elements with technological features (Table 7: ECN assemblage) continue with the dynamics of crafting lamellar flakes (n = 7) from different materials (two pieces of MP2 and one each of MP8, MP5, and MP10, respectively, with the rest unidentified) and the presence of a single crest on blade (MP6).

The presence of cortical pieces linked to materials MP6 (n = 3), MP2 (n = 2), and MP4 (n = 1), three on blades and five on flakes, is also noted.

Finally, we have only one microburin on the proximal part of a bladelet (11 mm width) made of material MP2.

4.3. Modified products

Morphological modification through retouching accounts for 31.83 % of the total artifacts, of which 56.42 % is observed on blades and 43.58 % on flakes, with some proportional and typological variability in the assemblages (Table 8 and Fig. 10). The proportions and combinations of retouch angles in each assemblage are specified in the supplementary table (see Table 5 supplementary material). Abrupt retouch (>50 %) predominates in all four assemblages, with a relatively lower proportion in ECN assemblage (<45 %), which shows a higher proportion of simple retouching and simple-abrupt combination retouching (both around 20–25 %).

4.3.1. Microlaminar Epipaleolithic tools

The retouched lithic assemblage from the Microlaminar Epipaleolithic levels (Interior-2, C5) consists of 53 artifacts, representing 25.6 % of the total assemblage.

The characteristic and predominant tools in the retouched assemblage are backed blades (maximum width 11.5 mm, with a predominance of 4–8 mm). Backed points on bladelets (n = 8) are remarkable, with both straight and curved backed edges, adding semi-oblique retouch on one or both ends. There are also two examples of oblique truncation. Due to the fracturing of these tools (four medial, six distal, and one proximal), only their generic categorization is possible, with only four complete pieces available.

The quantitatively significant modified products include endscrapers on both flakes and blades, showing abrupt or semi-abrupt retouch resulting in convex (n = 4 in each blank type) or concave fronts. The retouch can be either straight or sinuous, depending on the depth of potential wear from use (n = 1 in each case). There are also denticulates with marginal retouch (n = 7), including one with deep retouch, and three combined with isolated notches. Additionally, there are notches on blade (n = 4) and flake (n = 4) blanks, some of which are found on lamellar flakes and one on a cortical blade. Isolated notches are present on both flakes (n = 2) and blades (n = 3). There are also truncations on blades, and one on a bladelet, characterized by deep retouching and some very marginal retouch, resulting in various delineations of their ends (convex, straight, sinuous, or concave).

The remaining tools include a short-pointed perforator, an *écaillé* (or splintered) piece on a flake, a partially retouched flake with abrupt retouch, two partially retouched blades with simple retouch, and two cutting tools corresponding to a blade with truncation and lateral denticulate retouch.

4.3.2. Sauveterrian tools

The assemblage from Sauveterrian levels corresponds to 169 modified artifacts (32.06 %), 74 on flakes (43.78 %) and 95 on blades (56.21 %).

There is a noticeable change in morphotypes regarding typological proportions and the emergence of geometric forms in these levels. Backed blades and bladelets persist but in lower proportions compared to the previous assemblage. They are characterized by high fragmentation, with only one complete element, and the majority follow a microblade character (n = 17). Notably, there are a couple of backed points with distal points, one with an oblique truncation attached to the backed edge. Geometric forms are only sparsely present in this phase, with only one pygmy-sized segment (13 × 4 × 2 mm). However, complementary microburins to these productions appear, some with additional lateral retouch (n = 2), due to either later use or the reuse of the blade tool.

The rest of the modified pieces predominantly consist of denticulates on flakes (n = 24) and blades (n = 13), whether marginal or highly marginal compared to deep denticulations (n = 21 and 11, respectively), some combined with isolated notches (n = 4). Isolated notches (without denticulation) are produced exclusively on blades, some with lateral retouch interrupted by the notch (n = 1), or together with the presence of pseudo-retouch or micro-denticulations (n = 2). Other tools, such as endscrapers, display full convexity on their active edges. They appear on both flakes (n = 11) and blades (n = 7); in this latter case two tools possess a double edge (proximal–distal). Truncations are configured on blades (n = 11) and rarely on flakes (n = 2), some with partial truncations and one bitruncated blade, many of them showing lateral pseudo-retouches. The remaining tools are scarce but varied, including blade burins (one on a flake), a perforator on a flake (short tip), a sidescraper with simple marginal retouch, two blades with marginal retouch (bilateral and unilateral), and three *écaillé* pieces, one simple and the other two with flat retouch on flakes.

The assemblage reveals a series of tool reconfigurations (on blades, n = 12, and some small bladelets, n = 4), some corresponding to the rejuvenation of lateral edges (backed blades/denticulates, backed truncated blades, and notched truncations), as well as possible changes in the functionality of the tool itself (endscraper/denticulate and burin/notch). The remaining tools consist of simple partial retouches on primary blades and flakes.

4.3.3. Late Mesolithic tools

The modified tools in this phase represent 30.82 % of the assemblage, predominantly made on flakes (n = 24) rather than blades (n = 17). This time, there is a considerable decrease in the presence of projectile point production, and less specialized tools tend to be more representative.

The geometric characteristic is defined by an isosceles triangle with abrupt retouch (20 × 7 × 2 mm) and trapezoidal cross-section. It is complemented by the presence of six microburins (one medial and two proximal parts), one of which has complementary lateral retouch, as well as the presence of a notched configuration for blade fracture. Only one backed element is formed on a small blade (8.5 mm wide), preserving the medial part.

The rudimentary tools that predominate again are denticulates, notches, and endscrapers in equal proportions. Denticulates are mostly found on flakes (n = 4) and only one on a blade, with marginal denticulations on thin flakes (<8mm thickness) and a deep one on a thick flake. Isolated notches are found on both blades (n = 3) and flakes (n = 2). Burins are made on both blank types (three each), while other productions are exclusive to flakes. These include endscrapers (including three lamellar flakes), maintaining convex edges, except for one that is sinuous. Some combined morphotypes may indicate modification for passive and active use (truncate/notch) or for reuse (denticulate/opposite lateral retouch). Others are exclusively configured on blades, such as truncations, preferably oblique, although they are poorly represented.

4.3.4. Early Cardial Neolithic tools

The proportion of tools in the most recent phase represents 44.44 % of the total assemblage, predominantly on blades (n = 35) rather than on

Table 8
Number and percentage of morpho-techno-typological categories in each assemblage.

Morphologic and Typometric Categories	ME		SAU		LM		ECN	
	n	%	*n*	%	*n*	%	*n*	%
Geometric microlith	**0**	**0.00**	**1**	**0.59**	**1**	**2.44**	**5**	**8.33**
Trapeze	0		0		0		2	
Segment	0		1		0		3	
Triangle	0		0		1		0	
Backed blades/bladelets	**17**	**32.08**	**19**	**11.24**	**1**	**2.44**	**2**	**3.33**
Straight backed	13		13		1		2	
Arched backed	4		4		0		0	
SB/AB	0		2		0		0	
Perforators	**1**	**1.89**	**1**	**0.59**	**0**	**0.00**	**0**	**0.00**
Generic	1		0		0		0	
Spike	0		1		0		0	
Endscrapers	**11**	**20.75**	**18**	**10.65**	**5**	**12.20**	**3**	**5.00**
Thin flake endscraper (<8 mm thickness)	5		6		4		3	
Coarse flake endscraper (>8 mm thickness)	2		5		1		0	
Retouched blade endscraper	4		7		0		0	
Side scrapers	**0**	**0.00**	**1**	**0.59**	**0**	**0.00**	**0**	**0.00**
Side scraper with marginal retouch	0		1		0		0	
Truncations	**4**	**7.55**	**13**	**7.69**	**3**	**7.32**	**5**	**8.33**
Normal truncation	2		1		0		1	
Partial Normal truncation	0		3		1		2	
Oblique truncation	2		5		2		2	
Partial Oblique truncation	0		3		0		0	
Normal Bitruncation	0		1		0		0	
Denticulates	**9**	**16.98**	**37**	**21.89**	**5**	**12.20**	**21**	**35.00**
Marginal-very marginal denticulation	4		21		4		11	
Marginal/Deep denticulation	0		1		0		2	
Marginal denticulation/Simple notch	2		0		0		1	
Marginal denticulation/Retouched notch	1		3		0		1	
Deep denticulation	2		11		1		5	
Deep bilateral denticulation	0		1		0		0	
Deep/Marginal denticulation/Simple notch	0		0		0		1	
Notches	**5**	**9.43**	**18**	**10.65**	**5**	**12.20**	**8**	**13.33**
Simple Notch	1		3		0		1	
Simple bilateral notch	0		0		1		0	
Retouched Notch	4		12		4		5	
Retouched bilateral Notch	0		3		0		1	
Retouched Notch/Simple Notch	0		0		0		1	
Splintered pieces (*Écaillé*)	**1**	**1.89**	**3**	**1.78**	**0**	**0.00**	**0**	**0.00**
Retouch in extreme	0		1		0		0	
Retouch in lateral	1		2		0		0	
Burins	**0**	**0.00**	**6**	**3.55**	**6**	**14.63**	**2**	**3.33**
Angle burin	0		3		1		2	
Burin blow (generic)	0		2		4		0	
Double angle burin	0		1		0		0	
Double burin: angle and burin blow	0		0		1		0	
Microburins	**0**	**0.00**	**17**	**10.06**	**6**	**14.63**	**1**	**1.67**
Simple Notch	0		5		4		1	
Retouched notch	0		12		2		0	
Blades with marginal retouch	**0**	**0.00**	**2**	**1.18**	**0**	**0.00**	**6**	**10.00**
Unilateral retouch	0		0		0		4	
Bilateral retouch	0		2		0		2	
Retouched flakes	**1**	**1.89**	**18**	**10.65**	**7**	**17.07**	**1**	**1.67**
Thin flake (<8mm thickness)	1		16		5		1	
Coarse flake (>8mm thickness)	0		2		2		0	
Retouched blades	**2**	**3.77**	**1**	**0.59**	**0**	**0.00**	**0**	**0.00**
Unilateral	2		0		0		0	
Distal	0		1		0		0	
Composite tools	**2**	**3.77**	**14**	**8.28**	**2**	**4.88**	**6**	**10.00**
Endscraper/Denticulate	0		1		0		0	
Truncation/Denticulate	1		3		0		2	
Truncation/Notch	0		1		1		0	
Retouched flake/Burin	0		1		0		0	
Backed blade/Denticulate	0		1		0		1	
Backed blade/Truncation	0		6		0		1	
Burin/Notch	0		1		0		0	

(*continued on next page*)

Table 8 (*continued*)

Morphologic and Typometric Categories	ME		SAU		LM		ECN	
	n	%	*n*	%	*n*	%	*n*	%
Endscraper/Burin	0		0		0		1	
Denticulate/Burin	0		0		0		1	
Retouched flake/Denticulate	0		0		1		0	
Truncation/Denticulate/Blade with marginal ret.	1		0		0		0	
TOTAL	**53**	**100**	**169**	**100**	**41**	**100**	**60**	**100**

flakes (n = 25).

This time, the proportion of geometric microliths increases, corresponding to three segments with double bevel retouch and two trapezoids. One trapezoid has a retouch in the shorter base and a convex side, while the other has two concave sides. Both are created through abrupt retouching on both fractures, losing their microblade character (width 9.5–14 mm). It is worth noting the presence of one microburin and backed pieces, so scarcely detected in the previous assemblage.

Notches and denticulates predominate again, configured on both blades (n = 13) and flakes (n = 16). Denticulate pieces appear as marginal/very marginal (6 blades, 4 small blades, and 11 flakes), while notches are found on both blank types (5 flakes and 3 blades). They are made on the lateral edge, with one being bilateral and the other distal parts. Scrapers are less well represented, all on thin flakes with convex fronts, some of which have traces of ochre on the front. Reserved for flake productions, there is a simply retouched flake and two burins with a double burin blow (lateral angle). The remaining tools on blades include truncations (three on small blades), normal or oblique, all with straight edges, some with micro-retouches, and non-systematic lateral notches. There are also blades with marginal retouching, including simple unilateral and bilateral retouches. Finally, the composite tools include longitudinal cutting tools and possible modifications for hafting (Notch/Denticulate/Burin, Truncation/Denticulate, Truncation/Backed Blade), Backed Blade/Denticulate), and an object transformed into a burin (Scraper-burin) as a recycled tool.

5. Discussion

5.1. Variability of Cova del Vidre lithic assemblages

5.1.1. Sample and representativity considerations

Some general aspects that we must consider relate to issues regarding the representativeness of the analyzed sample. The first consideration is spatial and stratigraphic, as the representativeness of the recovered material is partial according to the extent of the excavated area related to the complete stratigraphy that may be present, along with the possibility of post-depositional or erosive disturbances that have not allowed the reliable inclusion of certain levels (EII, EIII, B1, and B2). The second pertains to assemblage preservation, including the high fracture index of the artifacts (>60 % in each assemblage) and the high tendency for thermal alterations, which hinder identification of the raw materials.

5.1.2. Raw material determination

The exploited raw material, predominantly flint, varies in the four phases but continuous parity exists between flint from carbonated lacustrine formations (medium–high quality) and evaporitic outcrops (medium–low quality). Some higher qualities of the latter seem to be selected and destined for blade and microblade production. Regarding the unknown origin of a specific material group, the blonde flint (G1), it has been detected at certain occupations in the Central-Southern Neolithic Ia, as in Abrigo de Falguera, Cova de l'Or, Cova de la Sarsa (Juan-Cabanilles, 1984; Asquerino et al., 1998; García-Puchol, 2005), and Cova de les Cendres (Bernabeu & Molina, 2009), among others. Moreover, an artifact in this material in the first occupation at Cova del Vidre would not be incongruous, as it has been documented in Early Holocene sites such as Tossal de la Roca (Cacho, 1990; Cacho et al., 1995), or even chronologically earlier in the Upper Paleolithic levels of Cova de les Cendres (Villaverde et al., 1999).

Outside this type of material of unknown geological formation and unknown radius of distance, the procurement of the raw materials in Cova del Vidre was generally local, combining nearby secondary outcrops in river valleys for both evaporitic and carbonated materials (<25 km), primary outcrops (<50 km), and some exogenous materials (G1, >100 km). A more detailed petrological and geochemical analysis could provide an in-depth understanding of the management, transformation, and circulation of these materials and their variability in each phase of occupation.

5.1.3. Technological variability and its relationship with raw material quality

There are several points to consider when comparing technological aspects among assemblages. Flake production dominates all analyzed assemblages except for ME, where laminar blanks prevail.

The larger flake productions are observed in the ME assemblage, means with 4–5 mm more in both length and width for the complete pieces. However, the fragmented pieces show less variability and are more similar among the four assemblages.

These data indicate the intense production following the small core sizes mentioned above. However, we can only define this pattern with certainty for SAU assemblage, as it is the only one with a quantitatively analysable sample of cores, albeit weakly represented.

According to the metric variables of length and width of the blanks (flakes and blades) and the application of statistical tests, we define H_0 as the homogeneity of values between assemblages. This hypothesis would expose the similarity of measurements of the exploited cores and/or nodules, as the implemented knapping strategies. By contrast, we suggest H_1 as the metric heterogeneity of these supports, which would indicate the existence of variability between assemblages. This could be associate to external factors and aspects, such as the type of material exploited in each assemblage, the different measurements of the exploited nodules and/or cores, and responding to different implemented knapping strategies.

Regarding this, the metric variability of the flake productions, the complete flakes from all assemblages (n = 181) show non-normal data distributions for both length (p-value = < 0.001) and width (p-value = < 0.001). Concerning the length data, we have the acceptance of H_1 (Kruskal-Wallis: p-value = 0.002792), and Dunn's test confirms the significance between the metrics of the ME and LM assemblages (p-value adj. = 0.0426) and the ME and SAU assemblages (p-value adj. = 0.00123). In this, it seems that ME assemblage flake length values tend to have a higher dispersion of data, mean and metric values than LM and SAU assemblages. For width measurements, H_1 is also accepeted (H_1, p-value = 0.03657), but the significance is only between the ME and LM assemblages (p-value. adj. = 0.0382), indicated also for the higher width values in ME assemblage confronting to LM assemblage.

Confirmed the normal distribution of their residuals (Shapiro-Wilk p-value: ME = 0.6371; SAU = 0.6371; LM = 0.2727; ECN = 0.28), a Simple Linear Regression of the width and length values of flakes in each assemblage provides a more precise understanding of the behaviour of these data. Two of the assemblages do not meet homoscedasticity: the

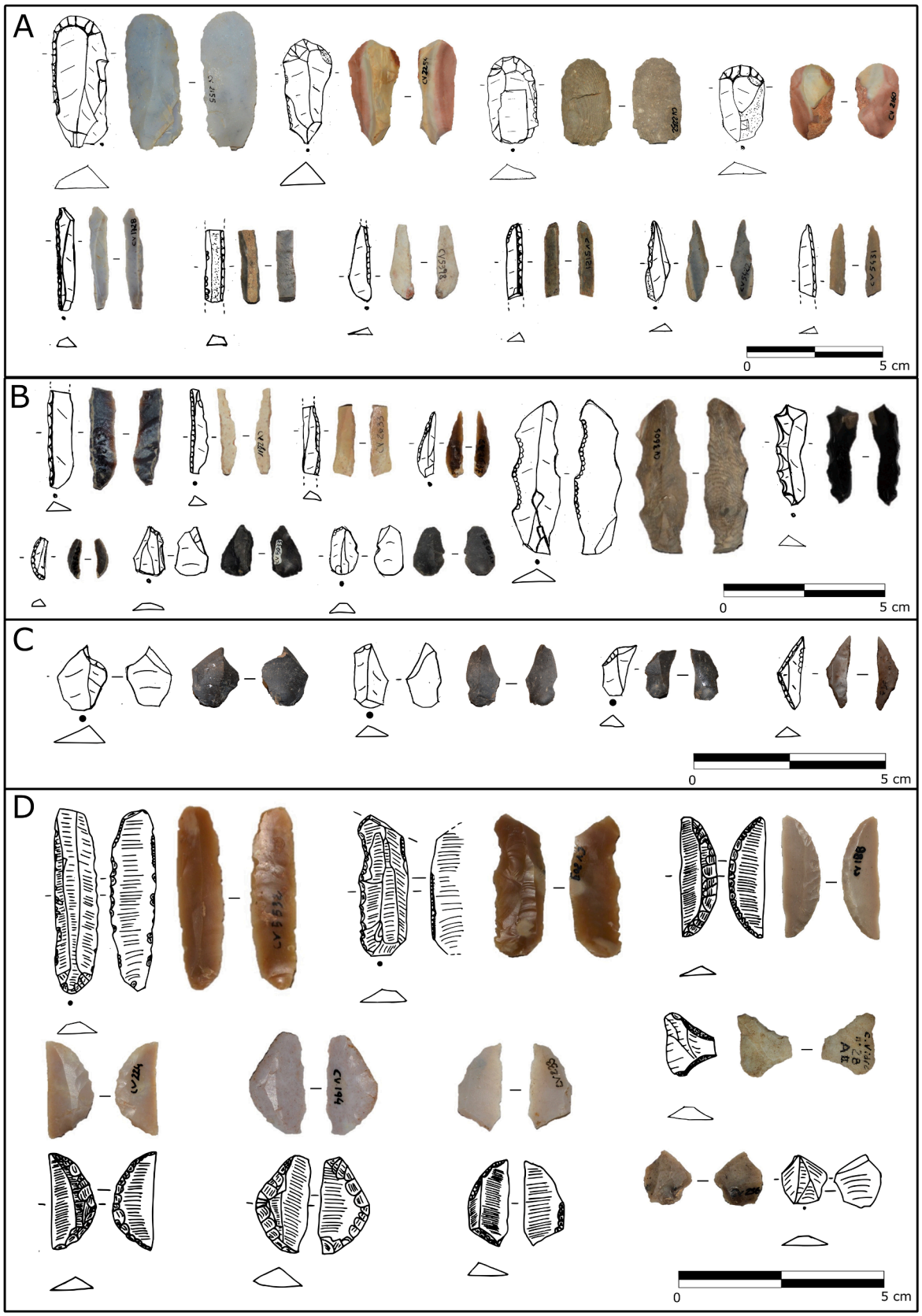

Fig. 10. Representative lithic techno-types in each assemblage (left to right/top–bottom): Endscrapers, backed bladelets and backed points (ME assemblage); Backed bladelets, backed points, denticulate blades, pygmy segment with abrupt retouch and microburins (SAU assemblage); Microburins and isosceles triangle with abrupt retouch (LM assemblage); Denticulate blades, geometric microliths (double-beveled retouch segments and abrupt retouch trapezes) and microburin (ECN assemblage). Drawings by J. Bosch.

ME assemblage (p-value = 0.032) and the SAU assemblage (p-value = < 0.001). The dispersion of the data in these two assemblages suggests that both regression models may be ineffective. In the other assemblages although the Simple Linear Regression models, explain less than 60 % of the data (ME = 56 %; SAU = 36 %; LM = 32 %; ECN = 6 %) there is, in general, an acceptance of a relationship between both variables with p-value < 0.05 and correlation strength of 0.95 (ME), 0.88 (SAU), and 0.61 (LM), except for the ECN set with p-value > 0.05 and weak correlation strength (0.27).

These data indicate metric homogeneity for complete flakes, remaining consistent in the ECN assemblage concerning ME, SAU, and LM. It reinforces the existing trend toward small-sized productions throughout the phases. The most notable differences in the length and width are observed between the ME and LM assemblages.

Additionally, despite considering the data dispersion issues introduced in the linear models and the unexplained variables, there are different rhythms. Length and width exhibit a positive trend, but the inclination is reduced over time: more pronounced in the Microlaminar Epipaleolithic than in the Early Cardial Neolithic (Fig. 11). However, we must consider the limited effectiveness of the models caused by other variables influencing these data (maybe raw material qualities, the weight of each piece, etc.), not explained in these models. These were not included in the analysis due to significant variability within these parameters and the sample-to-sample comparison between assemblages.

Regarding laminar productions, complete products show some variability in their averages. The ME assemblages maintains the highest values for both length and width, followed by the SAU assemblages, and finally, similar values between LM and ECN assemblages. Generally, all this data decrease over time. It is also noted in the averages of blades (fragments and complete) also showing a temporal decrease (the highest values in the ME assemblages, followed by SAU, LM, and finally, ECN).

If we apply a statistical comparison of the laminar blanks, we find non-normal distributions for complete blades (n = 68) in length (p-value = 0.01698) and width (p-value = < 0.001). On the one hand, the H_1 is established for length blades (p-value = 0.02381) between the ME and LM assemblages (p. adj. = 0.0185), but, on the other hand, H_0 is accepted for width values (p-value = 0.15). The same situation occurs with the width values of all blades (both fragmented and complete, n = 359, p-value = 0.13). Therefore, statistically, the metric length values of complete blades between ME and LM are significantly different. It is important to note that the length means for these assemblages are the highest and lowest, respectively, among the four assemblages (38.4 mm for the ME assemblage and 24.55 mm for the LM assemblage). However, this variability is not observed for widths (both complete and including fragmented ones).

According to the available data, excluding scarce or singular samples, there is a tendency towards a possible selection of raw materials for blade and bladelet products. Some material qualities are associated with microblades such as MP8 (present in LM and ECN assemblages) with an average width of around 10 mm, MP1 (ECN), and MP12 (SAU). MP2 is consistently present in all four assemblages, with average widths around 10–11 mm, although in variable proportions. It is worth noting that MP16 (found in ME and SAU assemblages) shows a slight increase in the width of blades in the later phase (B), while MP12 exhibits reduced width standards, indicating a greater focus on microblade reduction (SAU).

The comparison between blade blanks (fragmented and complete) and raw material quality (MP) indicate that the raw material does not influence the width of blades in the ME and LM assemblages (p > 0.05 in both cases). However, differences are established in the SAU and ECN assemblages: in the former between materials MP12 and MP5 (p-value. adj. = 0.0376) and in the latter between materials MP2 and MP8 (p-value. adj. = 0.0371). In both cases, the lowest mean values are established (MP12 in SAU and MP8 in ECN), and, by contrast, there is a trend

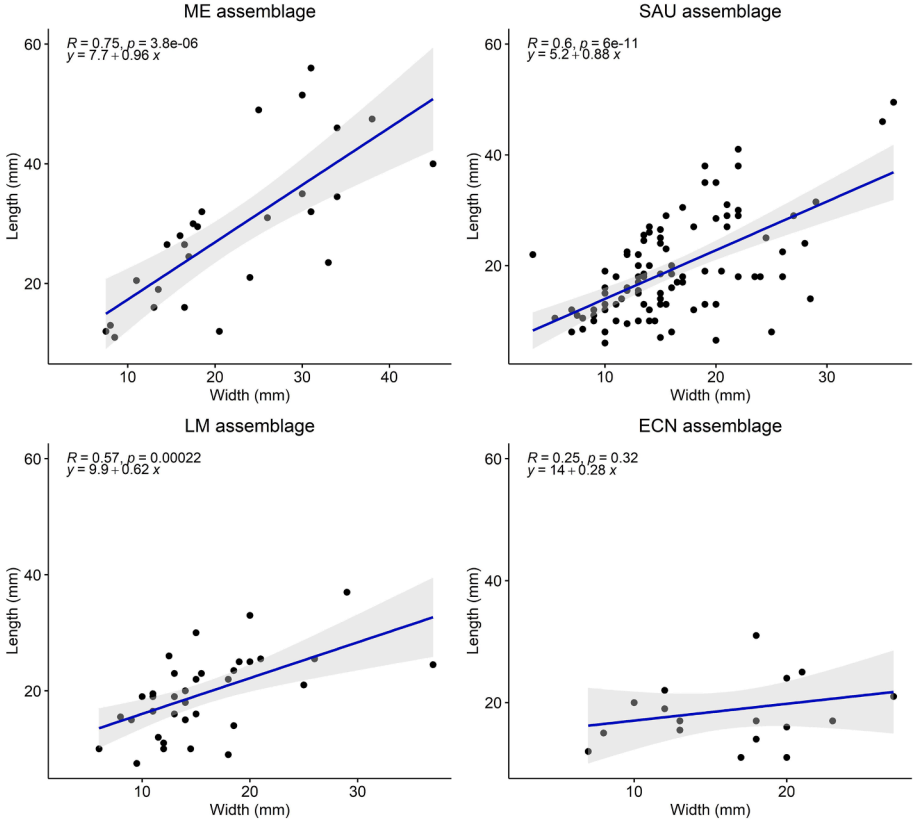

Fig. 11. Simple Linear Regression model of the length and width (mm) of complete flakes for each assemblage. We can observe non-proportional ascending between Length and Width (R= < 0.75) and the decreasing rhythm of Width confronting Length showing between assemblages.

towards higher mean widths (MP5 in SAU and MP2 in ECN).

A complementary point highlighted in this type of exploitation lies in the high representation of microlaminar blanks in the assemblages, even in the two most recent ones, exceeding 50 % of the laminar production. This could be attributed to exhaustive cores exploitation, although we have very limited samples (only acceptable number of samples in the SAU assemblage). However, the industry metrically indicates the exhaustion and amortization of cores due to maximum reduction. This trait is observed through the measurements of the products as well as the knapping errors that do not allow the continuity of core exploitation. At the same time, we can emphasize three possible causes that lead to these aspects: (1) The possible selection of materials destined for microlaminar production, which may be linked to a preference for specific attributes of the material itself that influence its quality. (2) The scarcity of a certain quality group of material, which, along with the possible existence of different levels of accessibility of these materials, technologically forces the exploitation of smaller nodules than in other types of qualities, also depending on their origin (primary or secondary). (3) According to mobility patterns, easy transport of nodules marked by their intensive exploitation, it also seems to have these same characteristics in the Neolithic phase. In this latter case, some of these aspects may be compatible with pastoral and hunting mobility (according to the geometric items available in the assemblage), considering its altitude (~1000 m above sea level) with short-duration occupations as an economic and strategic complement to those carried out in the river plain.

In these cases, we cannot firmly lean towards any of these scenarios (although they may also be combinable) due to issues related to both representativeness concerning the total analyzed assemblage (including unidentified MP's) and the variability in the sample size of artifacts linked to MP's.

5.1.4. Typological changes between phases

Tipologically, the retouched tools from the four phases maintain their differences according to the dynamics of neighboring occupations: in the ME and SAU assemblages, there is a significant predominance of endscrapers and backed blade elements, which together make up about 30–40 % of the toolkits. Secondarily, there is a notable representation of denticulates (15–20 %) and notches (~10 %). A distinction is established between them, introducing the first Sauveterrian geometric productions according to the pigmy segment and the significant quantity of microburins (~10 % for both).

From this point onward, the typological representation varies exponentially. This is particularly evident in the LM assemblage, where the proportions are distributed among more techno-types (burins, retouched flakes, notches, denticulates, endscrapers, all ranging between 12 and 17 %), along with a notable presence of microburins. Geometric elements stand out, along with the presence of a single geometric item, contrasting with the marked decline in backed blades, which are almost absent. In the ECN assemblage, there is another notable variation, with the near disappearance of microburins (see the next section for discussion), the predominance of denticulates (35 %), and a more numerous and morphologically variable presence of geometric pieces.

5.2. Macrospatial integration of Cova del Vidre: Lithic productions and chronostratigraphic sequence

Cova del Vidre gains relevance in the macro-regional framework due to its stratigraphic sequence and its lithic productions (Fig. 12). The oldest phase, based on the lithic assemblage and its radiocarbon date, is linked to an Epi-Magdalenian or Microlaminar Epipaleolithic (Bosch, 2005, 2016a) with its microlaminar industries spread across cave contexts. Locally, nearby Cova del Clot de l'Hospital (Bosch, 2005, 2016a; Bosch et al., 2015) exhibits the same production traits: backed points as projectile elements and standardized microblade productions corresponding to a single phase of occupation.

Within the surrounding area of El Port, the nearby site of La Roureda (Román, 2010) predates the Microlaminar Epipaleolithic at Vidre. The surrounding area of Serra del Montsant also exhibits different occupations that interact with these chronologies (Abric Filador levels 9–8; Abric de Sant Gregori; García Argüelles et al., 2005, 2020). Other sites around the Tarragona coastal and pre-coastal mountain range include Font Voltada (Mir & Freixas, 1993), Picamoixons (García Catalán et al., 2009), La Cativera (Morales et al., 2013b), and Molí del Salt (Asup level, Vaquero, 2004; García Catalán et al., 2013), as well as in the Maestrazgo region (Román & Domingo, 2017) with sites such as Cova dels Diablets (Aguilella et al., 2014), Cova dels Blaus (IVC level; Casabó, 2012), and Cingle de l'Aigua (level II, Villaverde et al., 2010; Román, 2010, 2011), all within this Late phase and exhibiting similar technological traits. Some of the similarities observed between the Vidre lithic assemblage and the ones at those sites can define generically the expansion of these traits, mainly associated with the predominance of backed pieces and endscrapers. This latter type of tool has certain techno-morphological similarities that indicate marked product standardization.

The industries in Sauveterrian, although represented by only one geometric element reinforced by the notable presence of microburins, are in line in terms of both production and chronology, according to the new radiocarbon date, with Levels 5–6 at Filador (García-Argüelles et al., 2005, 2013). Characteristically, the earlier microlaminar productions continue to be significant, and these new elements created using the microburin technique are incorporated for the first geometric pieces: abrupt segments and pygmy-sized scalene triangles, resulting from the same microlaminar productions and emerging from curved backed pieces (Román et al., 2021a, 2021b). It is important to emphasize the superposition of levels, as there is continuity between the microlaminar and geometric occupations, broadly observed in the case of Filador (García-Argüelles et al., 2005, 2013), or at sites on the Mediterranean coast, such as Balma del Gai (García-Argüelles et al., 2009); Can Sadurní (Fullola et al., 2011), or more inland sites like Cova del Parco (Fullola et al., 2002; García-Argüelles & Fullola, 2006), the latter presenting the oldest Sauveterrian assemblages according to its radiocarbon dates. This extension is also found on the eastern coast of the Iberian Peninsula, at such sites as Tossal de la Roca (Cacho et al., 1995) and Santa Maira (Aura et al., 2006).

The coexistence of Microlaminar and Sauveterrian industries is attested at the beginning of the Holocene in various occupations in the region. Contemporary with Microlaminar industries during the Younger Dryas, as seen in Cova del Vidre or Clot de l'Hospital (Bosch et al., 2015), the first geometric production emerges in contexts like Can Sadurní (21 (IVe)) (Fullola et al., 2011) and Cova del Parco (Ia2) (Fullola et al., 2002; García-Argüelles & Fullola, 2006), while the Microlaminar tradition persists into the Holocene, as seen in Cova de la Guineu (III) or Picamoixons (García-Catalán et al., 2009). The coexistence and continuity of these different industries in various contexts are often related to different technical or chrono-cultural traditions that spread across the territory (Cava, 2004). In parallel, the complexity of the productions during this transition from the Younger Dryas to the beginning of the Boreal period has been associated with technological and economic variability in response to climatic discontinuities, which eventually stabilized with the arrival of the climatic optimum around 8000 cal. BP (Soto et al., 2016; Bergadà et al., 2017; Aura et al., 2011; Dalmeri et al., 2004). These conditions directly impacted socio-economic and geostrategic aspects, leading to changes in human groups depending on the region, resulting from economic diversification at the time (Aura et al., 2009). This manifests as functional or seasonal variability in industries, even within the same groups (Morales et al., 2013b: 71).

The sequence documented in 1992 is interrupted after this point due to the separation of the two trenches, as the detected levels do not allow for a sequential bridge, resulting in a hiatus of 2952 years between the Sauveterrian and the Late Mesolithic based on the lower and upper limits of their calibrated dates, respectively. This occupational interruption, and the difficulty of associating other types of tools with a

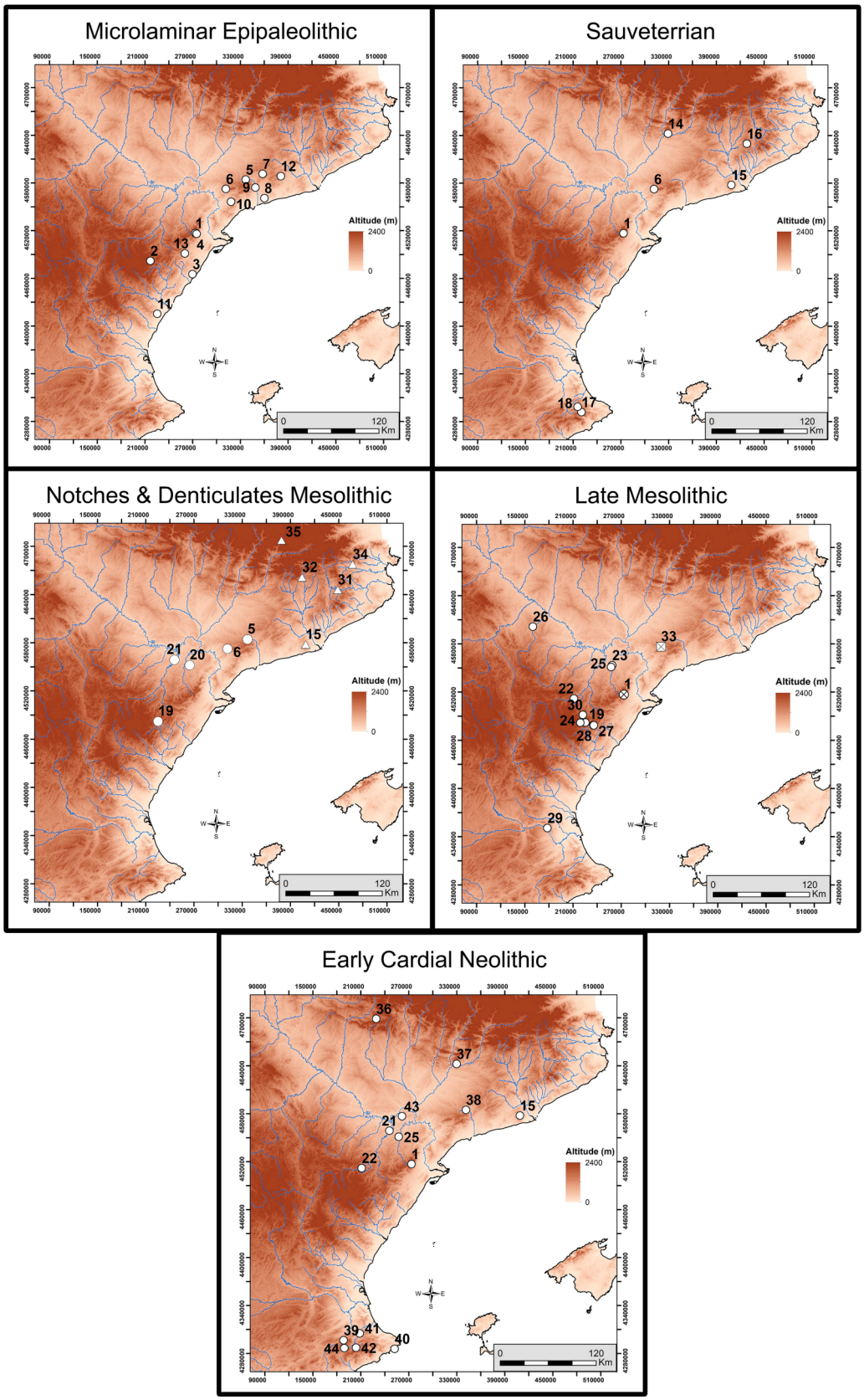

(caption on next page)

Fig. 12. Maps with the sites mentioned in text distributed chronologically: 1. Cova del Vidre; 2. La Roureda; 3. Cova dels Diablets; 4. Clot de l'Hospital; 5. Molí del Salt; 6. Filador; 7. Font Voltada; 8. La Cativera; 9. Picamoixons; 10. Sant Gregori; 11. Cova dels Blaus; 12. Cova de la Guineu; 13. Cingle de l'Aigua; 14. Cova del Parco; 15. Can Sadurní; 16. Balma del Gai; 17. Santa Maira; 18. Tossal de la Roca; 19. Balma Barranc de la Fontanella; 20. Costalena; 21. Plano del Pulido; 22. Abrigo de Ángel; 23. Abrigo de Pontet; 24. Abric de la Font d'Horta; 25. Botiquería dels Moros; 26. Cabezo de la Cruz; 27. Cingle del Mas Nou; 28. Cova Fosca; 29. Cueva de la Cocina; 30. Mas Cremat; 31. Roc del Migdia; 32. Font del Ros; 33. Coves del Fem; 34. Balma Serrat del Pont; 35. Balma Margineda; 36. Abrigo del Esplugón; 37. Abric del Xicotó; 38. Cova de la Font Major; 39. Cova de la Sarsa; 40. Cova de les Cendres; 41. Cova de l'Or; 42. Mas d'Is; 43. Valmayor XI; 44. Abric de la Falguera. In the Notches and Denticulates Mesolithic map, the sites with triangular icons are the occupations mentioned with recent radiocarbon dates or taphonomic issues between 6800 and 5700 cal. BC. In Late Mesolithic map, we point out Cova del Vidre as Geometric phase but without linking industrial subphase; and Coves del Fem with indetermined lithic technocomplex but located in the Ebro basin.

Notches and Denticulates Mesolithic techno-complex that may have experienced post-depositional movements, exclude, based on current evidence, the presence of such an occupation. However, they do appear in surrounding sites like Filador 2 (García-Argüelles et al., 2005) and Molí del Salt (Vaquero, 2004, 2006) in the northeastern Iberian Peninsula; Costalena (level d) and Plano del Pulido (level cm/cmp) in the Bajo Aragón region (Utrilla et al., 2009); or in a testimonial manner at Balma del Barranc de la Fontanella (Román & Domingo, 2021; Román et al., 2023) in the Alto Maestrazgo region.

When the focus is shifted to the record in the Central Sector of Cova del Vidre, the evidence becomes more complex. Firstly, there is a generalized issue in the northeastern Iberian Peninsula regarding the absence or less clear presence of the Late Mesolithic (c. 6800–5700 cal. BC). The few sites that may have occupation levels belonging to this chronological period present various challenges. Some have lithic productions that cannot be linked to neighboring regional dynamics, despite having radiocarbon dates within this range. Examples include Bauma Serrat del Pont (Alcalde & Saña, 2008), Font del Ros (Martínez-Moreno et al., 2006; Roda et al., 2016), and Roc del Migdia (Rodríguez, 1993; Rodríguez & Yll, 1991), while others face taphonomic issues related to Neolithic intrusions, such as Balma Margineda (Guilaine & Martzluff, 1995). Cova de Can Sadurní (Layer 20) falls within this timeframe (6290–6050 cal. BC, Bergadà et al., 2018), but detailed information about its lithic industry has not been published. In the southwestern part of the region, Cova del Vidre (Bosch, 2005, 2016a) and Coves del Fem (Bogdanovic et al., 2017; Palomo et al., 2018; Piqué et al., 2021) can be associated with the beginning and end of the Geometric Mesolithic phase, respectively. However, the lithic assemblages from these levels in the two sites do not exhibit the characteristics typical of these technocomplexes when compared to other sites of eastern Iberian Peninsula. The impact of the 8.2 Ka BP climatic event on human groups and other erosional factors, both natural and anthropogenic due to Neolithic settlement (Vaquero & García-Argüelles, 2009), have been the subject of debate about the affected populations. Additionally, a broader regional perspective considers the settlement dynamics of the Western Mediterranean and their connection to demographic gaps associated with the seasonal mobility of groups (González-Sampériz et al., 2009; Fernández-López de Pablo & Gómez-Puche, 2009; Vaquero & García-Argüelles, 2009; Bernabeu et al., 2018), which could be attributed to endogenous causes resulting in changes in social networks conditioned by Neolithic advancement (García-Puchol et al., 2009, 2015, 2022; García-Puchol & Salazar-García, 2017). The industrial characterization in these periods is closely related to our case study, and an extensive and systematic excavation that allows for a larger sample of material associated with this phase could elucidate its industrial relationship with neighboring contexts and its connection to the dynamics in the northeastern Iberian Peninsula, as well as Bajo Aragón and Maestrazgo. In the latter territories, occupations between 6200 and 5700 cal. BC are represented mainly by Botiquería (level 4), and in the Central Ebro basin by Cabezo de la Cruz (Rodanés & Picazo, 2013), while in the Maestrazgo region, sites such as Mas Cremat (Gabarda, 2010) and Cingle del Mas Nou (Olària & García, 2020) have been identified. Recent fieldwork around El Port also includes Balma del Barranc de la Fontanella (Román & Domingo, 2021; Román et al., 2023) and Abric de la Font d'Horta (Román & Domingo, 2022). However, the first has post-depositional issues (although the Cocina-type triangle Mesolithic is identifiable) and the second has a transitional Mesolithic-Early Cardial Neolithic radiocarbon date, without pottery but with lithic attributes that can correspond to the Neolithic period. In the case of Cova del Vidre, within this chrono-cultural panorama, it could be associated with the beginning of Phase B proposed for the Valencian region and defined mainly by the occupations of Cueva de la Cocina (Pardo-Gordó et al., 2018; García-Puchol et al., 2023; Juan-Cabanilles et al., in press), synchronizing with Abric del Pontet, even though the industry is associated with the A phase (Mazo & Montes, 1992). Alternatively, it could be chronologically aligned with the B phase, as seen in Cova Fosca IA and IB (Olària & Gusi, 1988; Llorente, 2010), Cingle del Mas Nou (Olària & García, 2020), and Coves del Fem (UE10) (Bogdanovic et al., 2017; Palomo et al., 2018; Piqué et al., 2021). However, the precise productive relationship remains to be determined, although these sites are closer to the dynamics of the Ebro basin and northern Levant due to the presence of geometric elements and the reinforcement of microburin technique attributes, also documented in the same phases at Botiquería (2 and 4), Pontet (e), and Ángel 1 (8c) (Utrilla et al., 2009). Further short-lived radiocarbon dates are expected to shed more light on the precise position of this Mesolithic evidence within this framework.

In the case of Cova del Vidre, despite the interruption in the 3-Central level and the approximate 710-year gap between the Mesolithic and Neolithic occupations, the typical continuity of geometric microliths and microburin technique in the latter period can be observed.

The presence of microburins proves to be conflicting according to their loss or general absence in the spatial and temporal framework we are dealing with. This distinguishes it from southeastern sites, which lack such productions in their occupations, as seen in Cova de l'Or, Cova de la Sarsa, Cova de les Cendres, Abrigo de Falguera, and Mas d'Is (Bernabeu & Molina, 2009:98), bending fracture being common (Juan-Cabanilles & Martí-Oliver, 2017:51). Other contexts with testimonial presence of microburins in the Neolithic phase include the cg level of Plano del Pulido (Utrilla et al., 2009), but intrusions from upper levels are exposed, and we lack any dating information. If we move away, pre-pyrenean contexts in the Neolithic levels of Abrigo del Esplugón (Utrilla et al., 2016) also show some presence. However, they are a scarce in these contexts. Faced with this situation, we will wait for more similar contexts to appear that may contain this type of geometric remnant and that can confirm more rigorously whether the microburin technique persisted during the Early Neolithic.

The presence of double-bevel retouch elements becomes normalized, particularly in segments corresponding to the second Cardial phase (~5240–5000 cal. BC; Oms et al., 2016), found in neighboring regions such as Botiquería 6 (Barandiarán, 1978; Utrilla et al., 2009) in Bajo Aragón, or Cova de la Font Major (Ig) (Cebrià et al., 2014) and Abric Xicotó (EC-3 II) (Oms et al., 2019) in the northeastern Iberian Peninsula. Other nearby sites also present these elements but within the range of the first Cardial phase (5600–5300 cal. BC), such as Abrigo de Ángel (2a1) (Domingo et al., 2010) or Valmayor XI-II (Rojo et al., 2015).

6. Conclusions

The comprehensive study of the lithic industry at Cova del Vidre, together with the new radiocarbon date obtained, has allowed us to define and include the stratified assemblages recovered by previous excavations within their corresponding chrono-cultural frameworks,

particularly in the case of the Sauveterrian assemblage and its temporal ascription.

Firstly, the heterogeneity of raw materials can be observed in both their acquisition and technological management, as well as in their intensive exploitation within the cave, indicated by the size of the lithic cores and the recycling of previously retouched artifacts. The presence of cortex on products and some cores suggests the transport of small natural nodules, although the possibility of transporting preformed or partially decorticated cores, as well as already formalized tools, is not excluded. Additionally, the production of the blades indicates a tendency to select certain materials for microlaminar production. Overall, the industry follows the same dynamics as the regional and supraregional technocomplexes, although the assemblage from the Late Mesolithic remains outside the comparative framework for now. However, it seems to approach the productive dynamics of the assemblages from the Bajo Aragón and Maestrazgo regions, rather than those in the northeastern Iberian Peninsula. This can be observed through the absence of the characteristic of the Notches and Denticulates Mesolithic macrotoolkit and the presence of blade production standardization, microburins, and an associated geometric component.

Secondly, the obtained radiometric date provides a reliable and accurate timeframe for the Sauveterrian within the 10th millennium cal. BC, allowing us to locate and contextualize the lithic assemblage recovered stratigraphically at the site in terms of production and territory. Additionally, we have gained a comprehensive understanding of the temporal sequence of the entire identified occupational history of the cave and its associated lithic productions. The interruption of the chronostratigraphic sequence at certain points may be influenced by erosive factors associated with specific climatic events that intensified water circulation and sedimentary erosion (e.g., 9.2 and 8.2 ky BP events), which could have resulted in (I) the destruction of occupation levels during this period; (II) the interior space becoming uninhabitable; or (III) external causes related to low accessibility and/or availability of subsistence resources. Regardless of these potential causes, which can only be determined through multidisciplinary studies, the sequential gaps of 2952 years between levels 1-Interior and 4-Central generally correspond to the chrono-cultural periods of the Notches and Denticulates Mesolithic and the Late Mesolithic Phase A. Additionally, there is a non-overlapped Neolithic occupation (710 years) without any transitional links between the last hunter-gatherer groups and the early agro-pastoral groups.

Future excavation work at the site, in addition to increased investment in a multidisciplinary analysis of the recovered remains and the integration of lithic data to other types of analysis and other materials (Nadal, 1998; Gibaja et al., 2018; Alcolea et al., 2022), will provide further insights and knowledge regarding the reconstruction of the occupational sequences at Cova del Vidre, the periods of abandonment, and the activities carried out at the site. It will also help clarify the paleoclimatic and sedimentological reconstruction of the site and its relationship with the duration of occupation and abandonment phases. This line of research will enable the integration of these data with aspects of the lithic assemblages, revealing the expansion of geometric technology from the Epipaleolithic to the Early Neolithic.

CRediT authorship contribution statement

Ivan Gironès-Rofes: Writing – review & editing, Writing – original draft, Visualization, Software, Project administration, Methodology, Investigation, Formal analysis, Data curation, Conceptualization. **Josep Bosch-Argilagós:** Writing – review & editing, Visualization, Validation, Supervision, Project administration, Investigation, Data curation. **Anna Bach-Gómez:** Writing – review & editing, Supervision, Project administration. **Miquel Molist:** Writing – review & editing, Supervision, Project administration. **Salvador Pardo-Gordó:** Writing – review & editing, Visualization, Supervision, Software, Resources, Methodology, Formal analysis, Data curation.

Declaration of competing interest

The authors declare that they have no known competing financial interests or personal relationships that could have appeared to influence the work reported in this paper.

Data availability

Code and all data used for this article can be found at https://doi.org/10.5281/zenodo.10161086.

Acknowledgments

This work is included in Departament de Cultura of Generalitat de Catalunya project 2022–2025 "*Evolució del poblament prehistòric al tram inferior de l'Ebre i al massís dels Ports*" (exp. 141). Acknowledgments to Museu de les Terres de l'Ebre (MTTE) with the director À. Farnós and the curator M. M. Villalbí and Museu de Tortosa with the director Maria José Lorenzo and the curator Eva Castellanos for the access to the artifacts studied in this work; and the investigators David Ortega and Xavier Terradas from IMF-CSIC to allow the access and consulting the lithoteque from the LITOcat project and their help; to Maria Saña and Vanessa Navarrete for the help received in the selection of faunal samples for 14C dating; and to Peter Smith and Roger Alcàntara for review some observations. Finally, very thanks to the anonymous reviewers, their comments have contributed positively to improving this paper.

Funding: IGR is the beneficiary of an FPI predoctoral contract (PRE2020-094236) in the framework of the Plan Estatal de Investigación Científica y Técnica y de Innovación 2017-2020 subject to the project PID-2019-106399GB-I00 with PI Miquel Molist Montaña. SPG is a beneficiary of Ramón y Cajal (RYC2021-033700-I) funded by MCIN/AEI/10.13013/501100011033. IGR, ABG and MMM are members of the research group supported by AGAUR-Generalitat de Catalunya: SGR 2021 00744. This work also has been included in the project CLT009/18100028 funded by AGAUR-Generalitat de Catalunya. Radiocarbon dates have been obtained in the context of the project PID2021-127141NA-I00 funded by *MCIN/AEI/10.13039/501100011033 and FEDER a way to make Europe*. Finally, funding from University of La Laguna and the Spanish Ministry of Universities is acknowledged.

Appendix A. Supplementary material

Supplementary data to this article can be found online at https://doi.org/10.1016/j.jasrep.2024.104408.

References

Aguilella, G., Roman, D., García, P. (Eds.), 2014. La Cova dels Diablets (Alcalà de Xivert, Castelló), Prehistòria a la Serra d'Irta, Servei d'Investigacions Arqueològiques i Prehistòriques, Diputació de Castelló.

Alcalde, G., Saña, M. (coords.), 2008. Procés d'ocupació de la Bauma del Serrat del Pont (La Garrotxa) entre el 5480 i el 7500 cal aC, Olot, Publicacions eventuals d'arqueologia de la Garrotxa 8, Museu Comarcal de la Garrotxa.

Alcolea, M., Chabal, L., Bosch-Arguilagós, J., Piqué, R., 2022. A southern refugium for temperate tree species in the Mediterranean mountains of El Port massif (NE Iberia): Charcoal analysis at Cova Del Vidre. The Holocene 32 (8), 794–806. https://doi.org/10.1177/09596836221095992.

Asquerino, M.D., López, P., Molero, G., Sevilla, P., Aparicio, M.T., Ramos, M.A., 1998. Cova de la Sarsa (Bocairent, Valencia). Sector 11: Gatera. Rec. Del Museu D'alcoi 7, 47–88.

Aura, J.E., Carrión, Y., García Puchol, O., Jardón, P., Jordá, J.F., Molina, L., Morales, J. V., Pascual, J.L., Pérez Jordá, G., Pérez Ripoll, M., Rodrigo, M.J., Verdasco, C., 2006. Epipaleolítico-Mesolítico en las comarcas centrales valencianas. In: Alday, A. (Ed.), El Mesolítico de muescas y denticulados en la cuenca del Ebro y el litoral mediterráneo ibérico. Memorias de yacimientos alaveses, 11. Vitoria: Diputación Foral Álava, pp. 65–118.

Aura, J.E., Jordà. J.F., Morales, J.V., Pérez, M., Villalba, M.P., Alcover, J.A., 2009. Economic transitions in finis terra: the western Mediterranean of Iberia, 15-7 ka BP. In: Before farming: the archaeology and anthropology of hunter-gatherers, University of Bristol Centre for Human Evolutionary Research, 2, 4.

Aura, J.E., Jordá, J.F., Montes, L., Utrilla, P., 2011. Human responses to Younger Dryas in the Ebro valley and Mediterranean watershed (Eastern Spain). Quat. Int. 242 (2), 348–359. https://doi.org/10.1016/j.quaint.2011.01.023.

Barandiarán, I., 1978. El Abrigo de la Botiquería dels Moros. Mazaleón (Teruel). Excavaciones Arqueológicas de 1974. Cuadern. Prehistoria Arqueol. Castell. 5, 49–138. http://hdl.handle.net/10234/45283.

Barceló, J.A., 2008. La seqüència cronocultural de la prehistòria catalana. Anàlisi estadística de les datacions radiomètriques de l'inici de l'Holocè a l'Edat del Ferro. Cypsela 17, 65–88.

Bartlett, M.S., 1937. Properties of sufficiency and statistical test. Proc. Roy. Soc. A 160, 268–282.

Bergadà, M.M., 1996. Estudio geoarqueológico de la secuencia holocena de la Cova del Vidre (Roquetes, Baix Ebre, Tarragona). I Congrés Del Neolític a La Península Ibèrica. Rubricatum I, 65–70.

Bergadà, M.M., Cervelló, J.M., Edo, M., Cebrià, A., Oms, F.X., Martínez, P., Antolín, F., Morales, J.I., Pedro, M., 2017. Chronostratigraphy in karst records from the Epipaleolithic to the Mid/Early Neolithic (c. 13.0–6.0 cal ka BP) in the Catalan Coastal Ranges of NE Iberia: environmental changes, sedimentary processes and human activity. Quat. Sci. Rev. 184, 26–46. https://doi.org/10.1016/j.quascirev.2017.09.008.

Bergadà, M.M., Cervelló, J.M., Edo, M., Antolín, F., Martínez, P., 2018. Procesos deposicionales y antrópicos en el registro holoceno de la Cova de Can Sadurní (Begues, Barcelona, España): aportaciones microestratigráficas. Boletín Geol. Minero 129 (1–2), 251–284. https://doi.org/10.21701/bolgeomin.129.1.010.

J. Bernabeu L. Molina (Eds.) La Cova de les Cendres (Moraira-Teulada, Alicante), Monografía Museo Arqueológico Provincial de Alicante (MARQ), Serie Mayor 2009 Alicante 6.

Bernabeu, J., Jiménez-Puerto, J., Escribá, P., Pardo-Gordó, S., 2018. C14 y poblamiento en las comarcas centro-meridionales del País Valenciano (c. 7000–1500 cal BC). Recerques Del Museu D'alcoi 27, 35–48.

Bogdanovic, I., Palomo, A., Piqué, R., Rosillo, R., Terradas, X. 2017. Los últimos cazadores-recolectores en el NE de la Península Ibérica: evidencias de ocupaciones humanas durante el VI milenio cal BC. In: Barceló, A., Bogdanovic, I., Morell, B. (Eds.), Actas del Congreso de Cronometrías Para la Historia de la Península Ibérica (IberCrono 2017). Universitat Autònoma de Barcelona, pp. 35–45.

Bosch, J., 1993. Cronologia prehistòrica al curs inferior de l'Ebre. Primeres Datacions Absolutes. Pyrenae 24, 53–56.

Bosch, J., 2001. Les ocupacions prehistòriques de caçadors-recolectors a la Cova del Vidre (Roquetes). Assent. Clima. Recerca 2001 (5), 9–20.

Bosch, J., 2005. El procés de neolitització a la regió del curs inferior de l'Ebre, Departament de Prehistòria, Història Antiga i Arqueologia. Universitat de Barcelona, Barcelona.

Bosch, J., 2011. La Cueva del Vidre (Roquetes, Bajo Ebro). Asentamiento del Mesolítico y del Neolítico Antiguo en la Cordillera Costera Catalana meridional. In: Gonçalves, V. S., Diniz, M., Sousa, A.C. (Eds.), 5°Congresso Do Neolitico Peninsular. Centro de Arqueologia da Universidade de Lisboa, Lisboa, pp. 182–188.

Bosch, J., Villalbí, M.M., Forcadell, A., 1996. El Barranc d'en Fabra (Amposta, Montsià): un assentament neolític a l'aire lliure. Tribuna D'arqueologia 1994–1995, 51–62.

Bosch, J., Nadal, J., Román, D., Estrada, A., 2015. Antiguas excavaciones, nuevas respuestas. El yacimiento epimagdaleniense de la Cova del Clot de l'Hospital (Roquetes, Baix Ebre). SAGVNTVM 47, 9–27. https://doi.org/10.7203/sagvntvm.47.3780.

Bosch, J., Clop, X., Gallart, J., Oms, F.X., 2022. El neolític antic a la conca catalana de l'Ebre: jaciments, ritmes i dinàmiques d'implantació i explotació del territori. Cypsela 22, 105–124.

Bosch, J., 2016a. Epipaleolític i neolític antic a la serra del Caro: les coves de l'Hospital i del Vidre (Roquetes, Baix Ebre). In: Martínez, J., Diloli, J., Villalbí, M. M. (coord.), Actes de les I Jornades d'Arqueologia de les Terres de l'Ebre. Tortosa, 1, pp. 63–77.

Bosch, J., 2016b. La cerámica de la Cova del Vidre (Roquetes) y el Neolítico Cardial Franco-Ibérico. In: Bonet, H. (coord.), Del neolític a l'edat de bronze en el Meditarrani occidental: estudis en homenatge a Bernat Martí Oliver. Serie de Trabajos Varios, Diputación Provincial de Valencia, Museu de Prehistòria de València, 119, pp. 109–116.

Breusch, T.S., Pagan, A.R., 1979. A simple test for heteroscedasticity and random coefficient variation. Econometrica 47, 1287–1294.

Brézillon, M., 1977. La dénomination des objets de Pierre taillée. Matériaux pour un vocabulaire des préhistoriens de langue française. CNRS, IV supplement à Gallia Préhistoire, Paris [2nd edition].

Cacho, C., Fumanal, M.P., López, P., López, J.A., Pérez Ripoll, M., Martínez Valle, R., Uzquiano, P., Arnanz, A., Sánchez Marco, A., Sevilla, P., Morales, A., Roselló, E., Garralda, M.D., García-Carrillo, M., 1995. El Tossal de la Roca (Vall d'Alcalà, Alicante). Reconstrucción paleoambiental y cultural de la transición del Tardiglaciar al Holoceno inicial. Recerques Del Museu D'alcoi 4, 11–101.

Cacho, C., 1990. Un premier essai d'étude des matières premières du Tossal de la Roca (Alicante, Espagne). In: Lenoir, M.; Seronie-Vivien, M. R. (Eds.), Le Silex de sa genèse à l'outil. Actes de V Colloque International sur le Silex. Cahiers du Quaternaire, 17, pp. 467–470.

Casabó, J., 2012. Las industrias de la Cova dels Blaus (La Vall d'Uixó, Castelló). Aportación a La Transición Paleolítico-Epipaleolítico En Las Comarcas Septentrionales Del País Valenciano, MARQ. Arqueología y Museos 5, 19–51.

Cava, A., 2004. Los procesos culturales del comienzo del Holoceno en la cuenca del Ebro y su contextualización. Salduie 4, 17–40.

Cebrià, A., Fontanals, M., Martín, P., Morales, J.I., Oms, F.X., Rodríguez-Hidalgo, A., Soto, M., Vergès, J.M., 2014. Nuevos datos para el Neolítico antiguo en el nordeste de la Península Ibérica procedentes de la Cova del Toll (Moià, Barcelona) y de la Cova de la Font Major (L'Espluga de Francolí, Tarragona). Trab. Prehist. 71, 134–145. https://doi.org/10.3989/tp.2014.12128.

Dalmeri, G., Ferrari, S., Perasani, M., 2004. Rise and fall in the utilization of trapezoidal microliths during the Late Upper Palaeolithic in Europe -an overview from the Italian Record. In: Terberger, T., Eriksen, B.V. (Eds.), Hunter in a Changing World Environment and Archaeology of the Pleistocene-Holocene Transition (ca 11000–9000 BC) in Northen Europe Rahden, Wesphalia, pp. 234–251.

Domingo, R., Bea, M., Utrilla, P., 2010. Una nueva ocupación neolítica en el río Guadalope: la campaña de 2009 en el abrigo de Ángel 2. Salduie 10, 225–235. https://doi.org/10.26754/ojs_salduie/sald.2010106617.

Dunn, O.J., 1964. Multiple comparisons using rank sums. Technometrics 6 (3), 241–252.

Esteve Gálvez, F., 2000. Recerques arqueològiques a la Ribera Baixa de l'Ebre. I: Prehistòria, Tarragona, Museu del Montsià-Ajuntament d'Amposta.

Fernández López de Pablo, J., Gómez Puche, M., 2009. Climate change and population dynamics during the late Mesolithic and the Neolithic transition in Iberia. Docum. Praehistor XXXVI, 67–96. https://doi.org/10.4312/dp.36.4.

Fortea, J., 1971. La Cueva de la Cocina. Ensayo de cronología del Epipaleolítico (Facies Geométrica). Trabajos Varios del SIP, 40. Servicio de Investigación Prehistórica. Diputación Provincial de Valencia, Valencia.

Fortea, J., 1973. Los complejos microlaminares y geométricos del Epipaleolítico mediterráneo español. Universidad de Salamanca, Salamanca.

Fullola, J., García Argüelles, P., Mangado, X., Medina, B. 2011. Paleolític i Epipaleolític al Garraf-Ordal. On érem i on som. In: Blasco, A., Edo, M., Villalba, M. J. (Eds.) La cova de Can Sadurní i la Prehistòria de Garraf. Recull de 30 anys dinvestigació. EDAR, Arqueología y Patrimonio, pp. 227–243.

Fullola, J.M., Petit, M.A., Bartolí, R., Nadal, J., Mangado, X., Calvo, M.A., 2002. Evolución de los sistemas de captación de recursos entre el Magdaleniense superior final y el Epipaleolítico geométrico de la Cueva del Parco (Alòs de Balaguer, La Noguera, Lleida). Zephyrus 55, 143–155.

Gabarda, M. V. (ed.), Hernández, F. J., Guillem, P. M., De Haro, S., Iborra, M. P., Martínez, R., Pérez, G., Pérez, R., Ruiz, J. M., Ten, S., Valcárcel, A. 2010. El cingle de Mas Cremat (Portell de Morella, Castelló). Un asentamiento en altura con ocupaciones del Mesolítico Reciente al Neolítico Final, Renomar S.A and Ein Mediterraneo S.L, Generalitat Valenciana.

García Argüelles, P., Fullola, J. M., Román, D., Nadal, J., Bergadà, M. M., 2013, El modelo epipaleolítico geométrico tipo Filador cuarenta años después: vigencia y nuevas propuestas. In: De La Rasilla, M., Homenaje a Javier Fortea Pérez., Ménsula Ediciones, Universidad de Oviedo, 151–165.

García Argüelles, P., Nadal, J., Roman, D., Lloveras, L., Bergadà, M. M., 2020. Las facies microlaminares del final del Paleolítico superior en el sur de Cataluña, in: Roman, D., García Argüelles, P., Fullola, J. M. (coords.), Las Facies microlaminares del final del Paleolítico en el Mediterráneo ibérico y el valle del Ebro. Societat Catalanad'Arqueologia, pp 117-147.

García Argüelles, P., Fullola, J.M., 2006. La cueva del Parco (Alos de Balaguer, Lleida) y el Abrigo del Filador (Margalef de Montsant, Tarragona): dos secuencias clave para el conocimiento del epipaleolitico en el Nordeste peninsular. Memor. Yacimientos Alaveses 11, 121–133.

García Argüelles, P., Nadal, J., Fullola, J.M., 2005. El abrigo del Filador (Margalef de Montsant, Tarragona) y su contextualización cultural y cronológica en el nordeste peninsular. Trab. Prehist. 62 (1), 65–83.

García Argüelles, P., Estrada, A., Fullola, J.M., Nadal, J., Mangado, X., 2009. Les niveaux épipaléolithiques de la Balma del Gai (Moià, Barcelone, Catalogne). In: Méditerranée Et D'ailleurs: Mélanges Offerts À Jean Guilaine. Archives d'Ecologie préhistorique, Tolouse, pp. 299–310.

García Catalán, S., Vaquero, M., Pérez Goñi, I., Menéndez, B., Peña García, L., Blasco, R., Mancha, E., Moreno, D., Muñoz Encinar, L., 2009. Palimpsestos y cambios culturales en el límite Pleistoceno-Holoceno: el conjunto lítico de Picamoixons (Alt Camp, Tarragona). Trab. Prehist. 66 (2), 61–76.

García Catalán, S., Gómez De Soler, B., Soto, M., Vaquero, M., 2013. Los sistemas de producción lítica en el Paleolítico superior final: el caso del nivel Asup del Molí del Salt (Vimbodí i Poblet, Tarragona). Zephyrus, LXXII, pp. 39–59.

García Puchol, O., Pardo-Gordó, S., Aura, J. E., Jordá, J. F., 2015. Last hunter-gatherers: Socioecological dynamics in Mediterranean Iberia. In: Bicho, N., Detry, C., Douglas Price, T., Cunha E. (Eds.), Muge 150th. The 150th anniversary of the discovery of Mesolithic shellmiddens. Cambridge Scholars Publishing, 2, pp. 93–107.

García Puchol, O., Salazar García, D.C. (Eds.), 2017. Times of Neolithic Transition along the Western Mediterranean. Springer.

García Puchol, O., Molina, L.L., Aura, J.E., Bernabeu, J., 2009. From the Mesolithic to the Neolithic on the Mediterranean coast of the Iberian Peninsula. Global action in human context. Adapting to the Holocene in Iberia. J. Anthropol. Res. 65, 2, 237–251. https://doi.org/10.3998/jar.0521004.0065.205.

García Puchol, O., Diez Castillo, A., Pardo-Gordó, S., Bernabeu Aubán, J., Cortell Nicolau, A., 2022. Assessing population dynamics in the spread of agriculture in the mediterranean iberia through early warning signals metrics. In: Pardo Gordó, S., Bergin, S. (Eds.), Simulating Transitions to Agriculture in Prehistory. Springer International Publishing, Cham, pp. 83–103.

O. García Puchol El proceso de neolitización en la fachada mediterránea de la península Ibérica 2005 Oxford.

O. García-Puchol S.B. McClure J. Juan-Cabanilles A. Cortell-Nicolau A. Diez-Castillo J.L. Pascual Benito M. Pérez-Ripoll S. Pardo-Gordó G. Gallello M. Ramacciotti L. Molina-Balaguer E. López-Montalvo J. Bernabeu-Aubán M. Basile C. Real-Margalef A. Sanchis-Serra Á. Pérez-Fernández T. Orozco-Köhler Y. Carrión-Marco G. Pérez-Jordà M. Barrera-Cruz P. Escribá-Ruiz J. Jiménez-Puerto A multi-stage Bayesian modelling for building the chronocultural sequence of the Late Mesolithic at Cueva de la Cocina (Valencia 2023 Quaternary International Eastern Iberia) 10.1016/j.quaint.2023.05.015.

Genera, M., 1993. Vinebre: Els Primers Establiments al riberal: recerques arqueològiques. Institut d'Estudis Tarraconses Ramon Brenguer IV, Diputació de Tarragona.
Genera, M., 1991. L'Ebre final: del Paleolític al món romà, Institut d'Estudis Dertosencs, 37, Tortosa.
Gibaja, J.F., Oms, F.X., Mestres, J., Mazzucco, N., Palomo, A., 2018. Primeros resultados sobre la función del utillaje lítico de las primeras comunidades neolíticas asentadas en Les Guixeres de Vilobí (Sant Martí Sarroca, Barcelona). SAGVNTVM-PLAV 50, 35–56. https://doi.org/10.7203/sagvntvm.50.11603.
Gironès, I., Molist, M., 2023. Palimpsestos, colecciones descontextualizadas y la estadística bayesiana: un punto de encuentro. Vegueta 23 (1), 187–241. https://doi.org/10.51349/veg.2023.1.07.
Gironès, I., Molist, M., Pardo-Gordó, S., 2020. Análisis tecno-tipológico y cronológico de la indústria lítica superficial recuperada en las terrazas del cauce del bajo Ebro. Zephyrus 86, 15–42. https://doi.org/10.14201/zephyrus2020861542.
Gironès, I., Bosch Argilagós, J., Gómez Bach, A., Molist Montaña, M., Pardo-Gordó, S., 2023. Variability and Temporality of Lithic Production in Epipaleolithic to Early Neolithic Occupations at Cova del Vidre (Catalonia. Zenodo, Spain).
González Sampériz, P., Utrilla, P., Mazo, C., Valero Garcés, B., Sopena, M.C., Morellón, M., Moreno, A., Martínez Bea, M., 2009. Patterns of human occupation during the early Holocene in the Central Ebro Basin (NE Spain) in response to the 8.2 ka climatic event. Quat. Res. 71, 121–132. https://doi.org/10.1016/j.yqres.2008.10.006.
Guilaine, J., Martzluff M., 1995. Les excavacions a la Balma de la Margineda (1979-1991). Estudi arquèologic (Govern d'A.). Andorra.
Juan Cabanilles, J., 1984. El utillaje neolítico en sílex del litoral mediterráneo peninsular. SAGVNTVM 18, 49–102.
Juan Cabanilles, J., Martí, B., 2002. Poblamiento y procesos culturales en la Península Ibérica del VII al V milenio a.C. (8000-5500 BP). Una cartografía de la neolitización. In: Bernabeu, J., Badal, E., Martí, B. (Eds.), El paisaje en el Neolítico Mediterráneo. SAGVNTVM-PLAV, Extra 5, pp. 45–87.
Juan Cabanilles, J., García Puchol, O., 2013. Rupture et continuité dans la néolithisation du versant méditerranéen de la péninsule Ibérique: mise à l'épreuve du modèle de dualité culturelle. In: Jaubert, J., Fourment, N., Depaepe, P. (Eds.), Transitions, Ruptures Et Continuité En Préhistoire: Évolution Des Techniques - Comportements Funéraires - Néolithique Ancien, Congrès Préhistorique De France. Éd. Société préhistorique française, Bordeaux, Paris, pp. 405–417.
J. Juan Cabanilles El utillaje de piedra tallada en la Prehistoria recinte valenciana Aspectos tipológicos, estilísticos y evolutivos, Serie de Trabajos varios, 109, Servicio de Investigación Prehistórica del Museo de Prehistoria de 2008 Valencia, Valencia.
Juan-Cabanilles, J., 1985. El complejo epipaleolítico geométrico (Facies cocina) y sus relaciones con el Neolítico antiguo. Sagvntvm 19, 9–30.
Juan-Cabanilles, J., Martí-Oliver, B., 2017. New Approaches to the Neolithic Transition: The Last Hunters and First Farmers of the Western Mediterranean, in: O. García-Puchol and D. C. Salazar-García (eds.), Times onf the Neolithic Transition along the Western Mediterranean. Fundamental Issues in Archaeology, Springer, 33-65. https://doi.org/10.1007/978-3-319-52939-4.
Juan-Cabanilles, J., García-Puchol, O., McClure, S. B., in press. Refining chronologies and typologies: Cueva de la Cocina (Dos Aguas, Valencia, Spain) and its central role in defining the Late Mesolithic sequence in the Iberian Mediterranean area. Quaternary International. https://doi.org/10.1016/J.QUAINT.2023.05.017 (2023).
Kenney, J. F., Keeping, E. S., 1962. Linear Regression and Correlation. Ch. 15 in Mathematics of Statistics, Pt. 1, 3rd ed. Princeton, NJ: Van Nostrand, 252-285.
Kruskal, W.H., Wallis, W.A., 1952. Use of ranks in one-criterion variance analysis. J. Am. Stat. Assoc. 47, 583–621. https://doi.org/10.1080/01621459.1952.10483441.
Lilliefors, H.W., 1967. On the Kolmogorov-Smirnov test for normality with mean and variance unknown. J. Am. Stat. Assoc. 62 (318), 399–402. https://doi.org/10.2307/2283970.
Llorente, L., 2010. The Hares from Cova Fosca (Castellón, Spain). Archaeofauna 19, 59–97.
Mangado, X., 2004. L'arqueopetrologia del sílex, una clau per al coneixement paleoeconòmic i social de les poblacions prehistòriques. Societat Catalana d'Arqueologia, Barcelona.
Martí, B., Aura, J., Juan Cabanilles, J.J., García, P.O., López, F., de Pablo, J., 2009. El Mesolítico Geométrico de tipo "Cocina" en el País Valenciano. In: Utrilla, P., Montes, L. (Eds.), El Mesolítico Geométrico En La Península Ibérica. Servicio de Publicaciones, Universidad de Zaragoza, Zaragoza, pp. 205–258.
Martínez Moreno, J., Casanova Martí, J., Mora, R., 2006. El Mesolítico de los Pirineos surorientales una reflexión sobre el significado de las facies de fortuna del postglaciar. In: Alday, A. (Ed.), El mesolítico de muescas y denticulados en la cuenca del Ebro y el litoral mediterráneo peninsular. Memoria de Yacimientos Alaveses, 11. Diputación Foral de, Álava, pp. 163–190.
Mazo, E., Montes, L., 1992. La transición Epipaleolítico - Neolítico antiguo en el yacimiento de El Pontet (Maella, Zaragoza), in Utrilla, P. (coord.), Aragón/Litoral Mediterráneo. Intercambios culturales durante la Prehistoria. Instituto Fernando el Católico, Zaragoza, pp. 243–254.
Mir, A., Freixas, A., 1993. La Font Voltada, un yacimiento de finales del Paleolítico Superior en Montbrió de la Marca (la Conca de Barberà, Tarragona). Cypsela, X 13–21.
Molist, M., Gómez, A., Borrell, F., Ríos, P., Bosch, J., 2016. El "Chassense" y los "Sepulcres de Fossa de Cataluña": relaciones complejas entre cultures arqueológicas vecinas, in Perrin, T., Chambon, P., Gibaja, J.F., Goude, G. (Dirs.), Le Chasséen, des Chasséens… Actes du colloque international de Paris (France). Archives d'Écologie Préhistorique, Tolouse, pp. 143–157.
Molist, M., Alcántara, R., Arnaiz, R., Gironès, I., Monforte Barberán, A., Sisa-López De Pablo, J., Piera, M., Vicens, L. V., Gómez Bach, A., 2020. Aportacions al coneixement de la prehistòria recent al tram inferior de la vall de l'Ebre (Móra la Nova, Benifallet, Aldover i Flix): dinàmica d'assentaments a l'aire lliure i en cova. Tribuna d'Arqueologia 2017-2018, Departament de Cultura, Generalitat de Catalunya.
Morales, J.I., Oms, X., 2012. Las últimas evidencias mesolíticas del NE Peninsular y el vacío pre-Neolítico. Rubricatum 5, 35–42.
Morales, J.I., Oms, F.X., Allue, E., Burjachs, F., 2013b. Le passage du Mesolithique aux premieres phases du Neolithique ancien dans le Nord-Est de la peninsule Iberique. Une problematique culturelle, ecologique et climatique. In: Jaubert, J., Fourment, N., Depaepe, P. (Eds.), Transitions, Ruptures Et Continuite En Prehistoire. Societe Prehistorique Française, Bordeaux, pp. 391–403.
Morales, I., Vergès, J.M., Fontanals, M., Ollé, A., Allué, E., Angelucci, D.E., 2013a. Procesos técnicos y culturales durante el Holoceno inicial en el noroeste de la Península Ibérica. Los niveles B y Bb de La Cativera (El Catllar, Tarragona). Trab. Prehist. 70, 1, 54–75. https://doi.org/10.3989/tp.2013.12102.
Nadal, J., 1998. Les faunes del Plistocè final-Holocè a la Catalunya Meridional i de Ponent: interpretacions tafonòmiques i paleoculturals. Universitat de Barcelona, Tesi doctoral.
Olària, C. R., García, F. R. 2020. Cingle del Mas Nou. Vida y muerte en el 7000 BP. Un campamento temporal del Mesolítico reciente, inmerso en los procesos de neolitización con inhumación colectiva (Parque rupestre de Gassulla. Ares del Maestre, Alto Maestrazgo, Castellón, España), Diputació de Castelló, Servei d'Investigacions Arqueològiques i Prehistòriques.
Olària, C.R., Gusi, F., 1988. Cova Fosca: un asentamiento meso-neolítico de cazadores y pastores en la serranía del Alto Maestrazgo. Servicio de Publicaciones, Diputación, D. L., Castellón.
Oms, F.X., Martín, A., Esteve, X., Mestres, J., Morell, B., Subirà, M., Gibaja, J., 2016. The neolithic in northeast iberia: chronocultural phases and 14C. Radiocarbon 58 (2), 291–309. https://doi.org/10.1017/RDC.2015.14.
Oms, F.X., Terradas, X., Morell, B., Gibaja, J.F., 2017. Mesolithic-Neolithic transition in the northeast of Iberia: chronology and socioeconomic dynamics. Quat. Int. 470/B, 383–397. https://doi.org/10.1016/j.quaint.2017.06.003.
Oms, F.X., Sánchez de La Torre, M., Petit, M.A., López-Cachero, F.J., Mangado, X., 2019. Nuevos datos del VI y V milenio cal BC en el llano y Prepirineo de Lleida: el Abric del Xicotó y Les Auvelles. Munibe 70, 93–107. https://doi.org/10.21630/maa.2019.70.05.
Ortega, D., Roqué, C., Terradas, X., 2016. Availability of siliceous rocks in the North-Eastern of Iberia: results from the LITOcat Project. In: Tarriño, A., Morgado, A., Terradas, X. (Eds.), Flint Geoarchaeology in Iberian Peninsula, vol. 26. University of Granada (CPAG 26), Granada, pp. 245–282.
Palomo, A., Terradas, X., Piqué, R., Rosillo, R., Bodganovic, I., Bosch, A., Saña, M., Alcolea, M., Berihuete, M., Revelles, J., 2018. Les Coves del Fem (Ulldemolins, Catalunya), Tribuna d'Arqueologia 2015–2016. Departament de Cultura, Generalitat de Catalunya, pp. 88–103.
Pardo-Gordo, S., García-Puchol, O., Diez, A., McClure, S.B., Juan-Cabanilles, J., Pérez Ripoll, M., Molina, L., Bernabeu, J., Pascual-Benito, J.L., Kennett, D.J., Cortell Nicolau, A., Tsantef, N., Basile, M., 2018. Taphonomic processes inconsistent with indigenous Mesolithic acculturation during the transition to the Neolithic in the Western Mediterranean. Quat. Int. 483, 136–147. https://doi.org/10.1016/j.quaint.2018.05.008.
Piera, M., Gómez, A., Molist, M., Ríos, P., Alcántara, R, 2016. El tram baix de l'Ebre a les èpoques del Neolític i Bronze inicial: Aportacions al seu coneixement a partir de l'assentament del Molló (Móra la Nova). In Martínez, J., Diloli, J., Villalbí, M. (coords.), Actes I Jornades d'Arqueologia de les Terres de l'Ebre. Tortosa, Generalitat de Catalunya, I, pp. 90–103.
Piqué, R., Palomo, A., Terradas, X., Andreaki, V., Barceló, J.A., Bogdanovic, I., Bosch, A., Gassmann, P., López-Bultó, O., Rosillo, R., 2021. Models of Neolithisation of the Northeastern Iberian Peninsula: new evidence of human occupations during the vi millennium cal BC. Open Archaeol. 7, 671–689. https://doi.org/10.1515/opar-2020-0153.
R Core Team R: A language and environment for statistical computing. R Foundation for Statistical Computing 2018 Vienna, Austria. <https://www.R-project.org/>.
Reimer, P.J., Austin, W.E.N., Bard, E., Bayliss, A., Blackwell, P.G., Bronk Ramsey, C., Butzin, M., Cheng, H., Edwards, R.L., Friedrich, M., Grootes, P.M., Guilderson, T.P., Hajdas, I., Heaton, T.J., Hogg, A.G., Hughen, K.A., Kromer, B., Manning, S.W., Muscheler, R., Palmer, J.G., Pearson, C., van der Plicht, J., Reimer, R.W., Richards, D.A., Scott, E.M., Southon, J.R., Turney, C.S.M., Wacker, L., Adolphi, F., Büntgen, U., Capano, M., Fahrni, S.M., Fogtmann-Schulz, A., Friedrich, R., K ̈ohler, P., Kudsk, S., Miyake, F., Olsen, J., Reinig, F., Sakamoto, M., Sookdeo, A., Talamo, S., 2020. The IntCal20 Northern Hemisphere Radiocarbon Age CalibrationCurve (0–55 cal kBP). Radiocarbon 62, 725–757. https://doi.org/10.1017/RDC.2020.41.
Rey-Solé, M., Román, D., Mangado, X., 2015. Aproximación al estudio arqueopetrológico de la industria lítica procedente del abrigo de La Roureda (Villafranca, Els Ports, Castelló, País Valencià). J. Lithic Stud. 2 (2), 119–143. https://doi.org/10.2218/jls.v2i2.1434.
Roda, X., Martínez Moreno, J., Mora, R., 2016. Ground stone tools and spatial organization at the Mesolithic site of font del Ros (southeastern Pre-Pyrenees, Spain). J. Archaeol. Sci. Rep. 5, 209–224. https://doi.org/10.1016/j.jasrep.2015.11.023.
Rodanés, J.M., Picazo, J.V., 2013. El campamento mesolítico del Cabezo de la Cruz (La Muela, Zaragoza), Monografías Arqueológicas/Prehistoria, 45. Universidad de Zaragoza, Zaragoza.
Rodríguez, A., 1993. L'Analyse fonctionnelle de l'industrie du gisement épipaléolithique/ mésolithique du Roc del Migdia (Catalogne, Espagne). Resultats Preliminaires. Préhistoire Européenne 4, 63–84.
Rodríguez, A., Yll, R., 1991. Materias primas y cadenas operativas en el yacimiento epipaleolítico de El Roc del Migdia (Barcelona). In: Mora, R., Terradas, X., Parpal, A.,

Plana, F. (Eds.), Tecnología y Cadenas Operativas Líticas. Treballs d'Arqueologia, I, 73–82.
Rojo, M., Tejedor, C., Peña Chocarro, L., Royo Guillén, J., Martínez, G., de Lagrán, I., Arcusa, H., Millán[a], M.S., Garrido, R., Gibaja, J., Mazzuco, N., Clemente, I., Mozota, M., Terradas, X., Moreno, M., Pérez, G., Álvarez Fernández, E., Jiménez, I., Gómez Lecumberri, F., 2015. Releyendo el fenómeno de la neolitización en el Bajo Aragón a la luz de la excavación del cingle de Valmayor XI. Zephyrus 75, 37–66. https://doi.org/10.14201/zephyrus2015754171.
Román, D., 2010. El jaciment Epimagdalenià de la balma de la Roureda (Vilafranca, Els ports, País Valencià). Pyrenae 41 (2), 7–28.
Román, D., 2011. Nuevos datos para la transición Pleistoceno Holoceno: el abrigo del Cingle de l'Aigua (Xert, Baix Maestrat, País Valenciano). Zephyrvs 66, 209–218.
Román, D., Domingo, I., 2017. El final del Paleolítico superior en Castellón: un territorio clave para la comprensión del final del Pleistoceno en el Mediterráneo ibérico. Pyrenae 48, 47–70.
Román, D., Domingo, I., 2019. Exploring the end of the upper magdalenian in northern Valencian region (Mediterranean Iberia). Quater. Int. https://doi.org/10.1016/j.quaint.2019.09.049.
Román, D., Domingo, I., 2021. Aportaciones al conocimiento del Mesolítico antiguo en la vertiente mediterránea de la península ibérica: la Balma del Barranc de La Fontanella (Vilafranca, Castelló). Trab. Prehist. 78 (2), 344–355. https://doi.org/10.3989/tp.2021.12280.
Román, D., Domingo, I., 2022. ¿Últimos mesolíticos o pioneros neolíticos? El Abrigo de la Font d'Horta (Vilafranca, Castelló, País Valenciano). Munibe Antropologia-Arkeologia 73. https://doi.org/10.21630/maa.2022.73.01.
Román, D., García Argüelles, P., Fullola, J. M., 2021b. La aparición de los elementos geométricos: el abrigo de El Filador (Tarragona) y su contextualización en el mediterráneo ibérico y el valle del Ebro. In: Bea, M., Domingo, R., Mazo, C., Montes, L., Rodanés, J. M. (Eds.). De la mano de la Prehistoria. Homenaje a Pilar Utrilla Miranda Monografías Arqueológicas. Prehistoria, 57, 341–360.
Román, D., García Argüelles, P., Nadal, J., Fullola, J.M., 2021a. The late microblade complexes and the emergence of geometric microliths in north-eastern Iberia. In: Boric, D., Antonovic, D., Mihailovic, B. (Eds.), Foraging assemblages. Serbian Archaeological Society The Italian Academy for Advanced Studies in America, Columbia University. Belgrade and New York, pp. 457–463.
Román, D., Domingo, I., Bergadà, M.M., Lloveras, L., Nadal, J., 2023. La Balma del Barranc de la Fontanella (Vilafranca, Castelló) y sus implicaciones en el conocimiento del Mesolítico Geométrico del Mediterráneo ibérico y el Valle del Ebro. Complutum 34 (1), 9–30. https://doi.org/10.5209/cmpl.88937.
Royo, J. I., Gómez, F., 1992, Riols I: Un asentamiento Neolítico al aire libre en la confluencia de los ríos Segre y Ebro, Aragón/ Litoral Mediterráneo: Intercambios Culturales durante la Prehistoria (P. Utrilla, coord.), Zaragoza, 297–308.
Shapiro, S.S., Wilk, M.B., 1965. An analysis of variance test for normality (complete samples). Biometrika 52 (3–4), 591–611. https://doi.org/10.1093/biomet/52.3-4.591.
Soto, A., Alday, A., Mangado, X., Montes, L., 2016. Epipaleolítico y Mesolítico en la vertiente sur de los Pirineos desde la perspectiva de la industria lítica. Munibe 67, 295–312. https://doi.org/10.21630/maa.2016.67.mis01.
Soto, A., Domingo, R., García-Simón, L.M., Alday, A., Montes, L., 2020. For a fistful of geometric microliths: reflections on the Sauveterrian industries from the upper and middle Ebro Basin (Spain). Quat. Int. 564, 61–74. https://doi.org/10.1016/j.quaint.2019.09.044.
Tixier, J., 1963. Typologie de l'Epipaléolithique du Maghreb. Arts et Métiers Graphiques. Mémoire du C.R.A.P.E.- Algeria, n° 2. París.
Utrilla, P., Montes, L., Mazo, C., Martínez Bea, M., Domingo, R., 2009. El Mesolítico Geométrico en Aragón. In Utrilla, P., Montes, L. (Eds.), El Mesolítico Geométrico en la Península Ibérica. Monografías Arqueológicas, 44, Universidad de Zaragoza, Zaragoza, pp. 131–190.
Utrilla, P., Berdejo, A., Obón, A. l., Laborda, R., Domingo, R., Alcolea, M., 2016. El abrigo de El Esplugón (Billobas-Sabiñánigo, Huesca). Un ejemplo de transición Mesolítico-Neolítico en el Prepirineo central, in Del neolític a l'edat del bronze en el Mediterrani occidental: estudis en homenatge a Bernat Martí Oliver, Serie de Trabajos Varios, 119, 75–96. Museu de Prehistòria de València, València. [On-line access: http://mupreva.org/pub/896/es].
Vaquero, M., García-Argüelles, P., 2009. Algunas reflexiones sobre la ausencia de Mesolítico geométrico en Cataluña, in: Utrilla, P., Montes, L., El mesolítico geométrico en la Península Ibérica. Monografías Arqueológicas, 44, 191–204.
Vaquero, M., 2004. Els darrers caçadors-recol·lectors de la conca de Barberà: El jaciment del Molí del Salt (Vimbodí). Excavacions 1999-2003, Museu Arxiu de Montblanc i Comarca. Montblanc.
Vaquero M., 2006. El Mesolítico de facies macrolítica en el centro y sur de Cataluña, in: A. Alday (coord.), El Mesolítico de muescas y denticulados en la cuenca del Ebro y el litoral mediterráneo peninsular. Vitoria, pp. 137–160.
V. Villaverde D. Román R. Martínez Valle M. Pérez Ripoll E. Badal M. Bergadà P.M. Guillem C. Tormo . in: Mangado, X. (coord.) El Paleolítico superior en el País Valenciano: Novedades y perspectivas 2010 Barcelona 8.
Villaverde, V., Martínez-Valle, R., Badal, E., Guillem, P., Garcia, R., Menargues, J., 1999. El Paleolítico superior de la Cova de les Cendres (Teulada-Moraira). Datos proporcionados por el sondeo efectuado en los cuadros A/B 17. Arch. Prehistoria Levantina XXIII, 6–65.